Effects of fluorine on the solubilities of Nb, Ta, Zr and Hf minerals in highly fluxed water-saturated haplogranitic melts

by

Abdullah Aseri

A thesis
presented to the University of Waterloo
in fulfillment of the
thesis requirement for the degree of
Master of Science
in
Earth Sciences

Waterloo, Ontario, Canada, 2012

AUTHOR'S DECLARATION

I hereby declare that I am the sole author of this thesis. This is a true copy of the thesis, including any required final revisions, as accepted by my examiners. I understand that my thesis may be made electronically available to the public.

Abstract

The effect of fluorine on the solubilities of Mn-columbite ($MnNb_2O_6$), Mn-tantalite ($MnTa_2O_6$), zircon ($ZrSiO_4$) and hafnon ($HfSiO_4$) were determined in highly fluxed, water-saturated haplogranitic melts at 800 to 1000 °C and 2000 bars. The melt corresponds to the intersection of the granite minimum with the albite-orthoclase tieline ($Ab_{72}Or_{28}$) in the quartz-albite-orthoclase system (Q-Ab-Or) due to the addition of P_2O_5 to the melt. The melt content of P_2O_5 is 1.7 wt. %, and also contains 1.1 and 2.02 wt. % of Li_2O and B_2O_3, respectively. The composition of the starting glass represents the composition of melts from which rare-elements pegmatites crystallized. Up to 6 wt. % fluorine was added as AgF in order to keep the aluminum saturation index (ASI) of the melt constant. In an additional experiment F was added as AlF_3 to make the glass peraluminous. The nominal ASI (molar Al/[Na+K]) of the melts is close to 1 and approximately 1.32 in peraluminous glasses, but if Li considered as an alkali, the ASI of the melts are alkaline (0.85) and subaluminous (1.04), respectively.

The solubility products $[MnO]*[Nb_2O_5]$ and $[MnO]*[Ta_2O_5]$ are nearly independent of the F content of the melt, approximately 18.19 ± 1.2 and 43.65 ± 2.5 $x10^{-4}$ K_{SP} (mol^2/kg^2), respectively. By contrast, there is a positive dependence of zircon and hafnon solubilities on the fluorine content, which increases from 2.03 ± 0.03 $x10^{-4}$ (mol/kg) ZrO_2 and 4.04 ± 0.2 $x10^{-4}$ (mol/kg) HfO_2 for melts with 0 wt. % F to 3.81 ± 0.3 $x10^{-4}$ (mol/kg) ZrO_2 and 6.18 ± 0.04 $x10^{-4}$ (mol/kg) HfO_2 for melts with 8 wt. % F. Comparison of the data from this work and previous studies indicates that ASI of the melt seems to have a stronger effect than the contents of fluxing elements in the melt and the overall conclusion is that fluorine is less important (relative to melt compositions) than previously thought for the control on the behavior of high field strength elements in highly evolved granitic melts.

Moreover, this study confirms that although Nb, Ta, Zr and Hf are all high field strength elements, Nb-Ta and Zr-Hf are complexed differently.

Acknowledgements

I would like to thank my supervisor Dr. Robert Linnen for his support, patience and advice during the program period. I would also like to thank my thesis committee members Dr. Eric J. Reardon, Dr. Shoufa Lin and Dr. Mario Coniglio

Also I like to thank Yves Thiboult for his assistance in microprobe analysis at CANMET. During my work, I have met many friends who helped me and provided valuable advice. They include Ahmed Wasfy, Alaa Alturk, Hassene Bouraoui, Fahad Al-zahrani and Xu Dong Che.

Special thanks to my father and mother, who have been praying for me since the day I left home, and to my brothers and sisters.

Thanks to King Abdul Aziz University for giving me the opportunity to continue my graduate study, and also to Dr. Orfan Shouaker-Stash, Dr. Saleh Bajaba, Dr. Talal Qadi and Dr. Hesham Harbi, who provided me with advice and support.

Table of Contents

List of Figures

List of Tables

Chapter 1
Introduction

1.1 Geochemistry background

Niobium (Nb), tantalum (Ta), zirconium (Zr) and hafnium (Hf) are classified with high field strength elements (HFSE), because these elements have high charge to ionic radius. As consequence they are incompatible with the most rock forming-minerals, thus, in magmatic systems they concentrate in residual melts until the saturation of an accessory phase. These elements received an enormous amount of attention for their importance in electronics, aerospace, optic and other modern technology industry (Agulyansky, 2004). In particular, many investigations have studied the enrichment and behavior of these elements during magma evolution (Cerny et al., 1985; Hofmann, 1988; Keppler, 1993; Linnen and Keppler, 1997; 2002; Hui et al., 2010).

1.1.1 Niobium and Tantalum

Niobium and tantalum are located in group 5 in the periodic table (or V-A in older IUPAC periodic table). They both have a 5^+ charge and similar ionic radius (Table 1-1). They are incompatible elements in magmatic systems (Linnen and Keppler, 1997), and due to the identical chemical properties of Nb and Ta (Table 1-1), Nb/Ta ratio should remain constant and equal to their ratio in the most unfractionated rocks (carboniferous chondrite, Hui et al., 2011). However, Nb/Ta ratio in oceanic crust is not consistent and shows subchondritic values, and in upper continental crust, Nb/Ta ratio is extremely low (≈11, Cerny et al., 1985).

Several studies have investigated why the Nb/Ta ratio in upper crust rocks and some basalts are non-chondritic. Although oceanic basalts should have chondritic value, mid oceanic ridge basalt (MORB), back arc basin basalt (BABB) and oceanic island basalt (OIB) have different Nb/Ta ratios and they are all subchondritic values (Hui et al., 2011). That indicates that the mantle sources of these basalts must have subchondritic values (Rudnick et al., 2000). The correlation between Nb/Ta ratio

and the ratios of more incompatible elements over less compatible elements (La/Sm, Rb/Cs, Nb/U), as well as the correlated variations between Nb/Ta and Zr/Hf in lunar rocks and abyssal peridotites are consistent with a magmatic origin for fractionation of Nb and Ta from magmatic origin (Hui et al., 2011). This conflicts with the previous concept that Nb-Ta and Zr-Hf pairs cannot be fractionated readily by geochemical processes. Consequently, other factors were proposed to explain Nb-Ta and Zr-Hf fractionation such as mass dependent fractionation, electron configuration-dependent and metasomatic processes (Hui et al., 2011).

Pfander et al., (2012) reported high Nb/Ta ratio (higher than oceanic basalt value) in continental alkaline basalt from Central Germany. This value (19.1) is also higher than the average Nb/Ta ratio in continental crust (12 to13). These high Nb/Ta domains were explained by being restricted to regions that have been affected by carbonatite metasomatism. Keppler (1996) showed that calc-alkaline basalts are depleted in Nb-Ta, but are enriched in large ionic lithophile elements (LILE). This characteristic was attributed to chemical transportation of LILE by an aqueous fluid.

Linnen and Keppler (1997) reported that molar solubility of Mn-tantalite (MnTa2O6) is more soluble than Mn-columbite (MnNb2O6) in subaluminous to peraluminous melts, whereas in peralkaline melts their molar solubilities are nearly equal. Linnen and Keppler (1997) reported that molar solubility of Mn-tantalite (MnTa2O6) is more soluble than Mn-columbite (MnNb2O6) in subaluminous (ASI, alumina saturation index, molar Al/[Na+K] = 1) to peraluminous melts (ASI>1), whereas in peralkaline melts (ASI<1) their molar solubilities are nearly equal. Thus, the differences in Nb and Ta contents cause dramatic changes in the Nb/Ta ratio (Cerny, 1985a). Wang et al. (1982) showed that Nb- and Ta-fluorine complexes have different thermal stabilities. Ta-fluorine complexes are more stable to lower temperature than Nb-bearing complexes. Therefore, Nb tends to crystalize

from the melt in earlier. Consequently, the changes in the Nb/Ta ratio can be attributed to their different thermal stabilities at different temperatures of during the cooling of magmas.

1.1.2 Zirconium and Hafnium

Zirconium and hafnium are group 4 elements in the periodic table (or V-A in older IUPAC periodic table). They both have 4^+ charge and have similar ionic radius (Table 1-1), and due to the high charge to ionic radius ratio they are classified with HFSE. Although the ionic radius of Hf is smaller than Zr, and has lower ionization potential and electronegativity, the Zr-Hf pair considered as one of the most coherent geochemical pairs (Cerny, 1985a). Therefore, because of their incompatibility and the similarities, Zr/Hf should be constant during magma evolution from mafic to felsic. However, the Zr/Hf ratio is not constant and becomes either higher (in some oceanic basalts. i.e. interpolate basalts of Nyiragongo, DR. Congo) or lower (in granitic rocks) than the chondritic values (Dupuy, 1992). The high Zr/Hf ratio can be explained as a result of fractionation of clinopyroxene (David et al., 2000). Low Zr/Hf ratio in granitic rocks has been attributed to fluid metasomatism (Hildreth, 1979, 1981; Bau, 1996), or to crystal fractionation (Linnen and Keppler, 1997; Pan, 1997).

1.2 HFSE in Rare elements pegmatite rocks

Generally, HFSE, as well as rare earth elements (REE), are associated with highly evolved peralkaline and peraluminous granites. Because of the high concentrations of these elements in these kinds of rocks, they are also known as rare element granites and pegmatites (Linnen and Cuney, 2005). Rare element pegmatites represent the latest and most fractionated stages of magmatic sequences. Based on their contents of rare elements, rare element pegmatites are classified by Cerny and Ercit (2005) into two families, the NYF (Nb, Y and F) and LCT (Li, Cs and Ta) families. The NYF family is characterized by Nb > Ta (Cerny and Ercit, 2005; Linnen and Cuney, 2005) and this

suite of elements is also typical of A-type granites (Collins et al. 1982). In addition to the high concentration of Nb, Y and F, they are enriched in heavy rare-earth elements (HREE), Sc, Zr, Be and Ti (London, 2008). The LCT family is more abundant and generally they associated with S-type granites (Chappell and White, 1991). However, similar enrichments can also be found in I-type granites such as the Mole granite, Australia (Cerny, 1991a). Pegmatites that belong to this family are enriched in Be, B, F, P, Mn, Ga, Rb, Nb, Sn and Hf, in addition to Li, Cs and Ta (London, 2008). Deposits of HFSE belonging to this family can contain several hundred ppm of Ta to a few wt. % of Nb and Zr, whereas primitive mantle (PM) contains 0.588 ppm Nb, 0.040 ppm Ta, 10.8 ppm Zr and 0.300 ppm Hf (Palme and O`Neill, 2004), and 12 ppm Nb, 8 ppm Ta, 132 ppm Zr and 3.7 ppm Hf, in the upper crust (Rudnick and Gao, 2004). Therefore, in order for HFSE to reach these high concentrations in ore deposits, the enrichment factors of these elements would range from 1000 to 50,000 (Linnen et al., in press)

1.3 The role of fluxing elements

Rare elements pegmatites are a major source for HFSE deposits. The enrichment of HFSE in rare metal granites and pegmatites is usually associated with elevated concentrations of F and the other fluxing components such as Li, B, P and H_2O (Linnen, 1998). Thus, understanding the effect of flux elements on the behavior of HFSE in granitic melts is crucial.

The effects of fluxing elements on the solubilities of Nb, Ta, Zr and Hf accessory phases have been the subject of many studies. Linnen and Keppler (1997) showed that Nb and Ta solubilities in subaluminous and peraluminous melts increase with increasing water content from 0 to 3 wt. %. By contrast, water has no effect on the Nb and Ta solubilities in peralkaline melts, which was confirmed by Bartels et al. (2010). Similarly, Linnen (2005) reported that the accessory phases of Nb, Ta, Zr, Hf, Ti and W are not affected by water content of peralkaline melts. By contrast, the solubilities of

accessory phases in subaluminous melts increase with water content up to 2 wt. %. At higher water contents, the solubilities are nearly constant (Linnen, 2005).

The solubility of tantalite increases by factor of 2 to 3 with the addition of 2 wt. % Li2O in granitic liquids that have a Li-ASI (molar Al/[Na+K+Li]) of 1 at 750 to 1035 °C and 2 kbars (Linnen, 1998; Bartels et al., 2010). By contrast, Zr and Hf solubilities decrease with increasing Li concentration in the melts, which was attributed to the low field strength of Zr^{4+} and Hf^{4+} compared to Nb^{5+} and Ta^{5+}, and that affects their ability to compete with Li for non-bridging oxygen tetrahedra (NBO) which is not shared by two silicon (Linnen, 1998).

Bartels et al. (2010) reported that the presence of P and B in granitic melts should also increase the solubilities of Mn-columbite and Mn-tantalite. However, Wolf and London (1993) suggested that phosphorous only increases columbite solubility, whereas boron appears to have no effect.

Fluorine's effect on the solubility of Nb, Ta, Zr and Hf is controversial. Keppler (1993) reported that the solubilities of HFSE minerals increase with increasing F content in the melt. The increase of HFSE minerals solubilities was explained by increasing the number of NBO in the melt due to the reaction of F with Al to form AlF_6^{-3}complexes. Keppler (1993) also suggested a direct complexing of HFSE and F in the granitic melts, to explain the increase in their solubilities. However, based on the analysis of the local environment around Zr using XAFS analysis (X-ray absorption fine structure), Farges (1996) showed there is no clear evidence for F first neighbors around Zr in F-bearing albitic glass. Nevertheless, the study confirms the effect of F on the local environment around Zr. Van Lichtervelde et al. (2010) concluded that F has a weak effect on Mn-tantalite and zircon solubilities. By contrast, Fiege et al. (2011) showed that F has no effect on the solubilities of Mn-columbite and Mn-tantalite in subaluminous haplogranitic melts. Moreover, Baker and Conte (2002) reported that adding 0.35 wt. % Cl or 1.2 wt. % F to peralkaline melts has a weak effect on both

solubility and diffusivity of Zr in nearly water saturated metaluminous granitic melts at 1,200 and 1,050 °C, and at 1 kbar.

1.4 Objectives

Fluorine is one of the fluxing elements that commonly exist in high levels in association with HFSE deposits. As shown above, the effect of F on the solubilities of HFSE accessory minerals is controversial. Furthermore, there are no studies in the literature focusing on the effects of F on the solubilities of HFSE minerals in highly fluxed haplogranitic melts. Therefore, the effects of fluorine levels on the solubility of Nb, Ta, Zr and Hf minerals will be investigated, as well as temperature and the melt aluminum saturation index (ASI, molar Al/[Na+K]).

1.5 Thesis layout

This thesis consists composed of two chapters. The first chapter is a general introduction to chemistry and geochemistry of HFSE, as well as their behavior during magma evolution. Furthermore, some experimental investigations on the behavior of HFSE at variable conditions (temperature, pressure and melt composition) are reviewed. Chapter 2 was written as independent paper, which has its own abstract and introduction. This chapter investigates the fluorine effect on the solubilities of Mn-columbite, Mn-tantalite, zircon and hafnon in highly fluxed haplogranitic melts. Moreover, the effect of temperature on the solubilities of the aforementioned minerals will be investigated as well as the effect of ASI.

Chapter 2

Effects of fluorine on the solubilities of Nb, Ta, Zr and Hf minerals in highly fluxed water-saturated haplogranitic melts

2.1 Overview

The effect of fluorine on the solubilities of Mn-columbite ($MnNb_2O_6$), Mn-tantalite ($MnTa_2O_6$), zircon ($ZrSiO_4$) and hafnon ($HfSiO_4$) were determined in highly fluxed, water-saturated haplogranitic melts at 800 to 1000 °C and 2000 bars. The melt corresponds to the intersection of the granite minimum with the albite-orthoclase tieline ($Ab_{72}Or_{28}$) in the quartz-albite-orthoclase system (Q-Ab-Or) due to the addition of P_2O_5 to the melt. The melt content of P_2O_5 is 1.7 wt. %, and also contains 1.1 and 2.02 wt. % of Li_2O and B_2O_3, respectively. The composition of the starting glass represents the composition of melts from which rare-elements pegmatites crystallized. Up to 6 wt. % fluorine was added as AgF in order to keep the aluminum saturation index (ASI, molar Al /[Na+K]) of the melt constant. In an additional experiment F was added as AlF_3 to make the glass peraluminous. The nominal ASI of the melts is close to 1 and approximately 1.32 in peraluminous glasses, but if Li considered as an alkali, the Li-ASI (Al /[Na+K+Li]) of the melts are alkaline (0.85) and subaluminous (1.04), respectively.

The solubility products $[MnO]*[Nb_2O_5]$ and $[MnO]*[Ta_2O_5]$ are nearly independent of the F content of the melt, approximately 18.19 ± 1.2 and 43.65 ± 2.5 $x10^{-4}$ K_{SP} (mol^2/kg^2), respectively. By contrast, there is a positive dependence of zircon and hafnon solubilities on the fluorine content, which increases from 2.03 ± 0.03 $x10^{-4}$ (mol/kg) ZrO_2 and 4.04 ± 0.2 $x10^{-4}$ (mol/kg) HfO_2 for melts with 0 wt. % F to 3.81 ± 0.3 $x10^{-4}$ (mol/kg) ZrO_2 and 6.18 ± 0.04 $x10^{-4}$ (mol/kg) HfO_2 for melts with 8 wt. % F. Comparison of the data from this work and previous studies indicates that ASI of the melt

seems to have a stronger effect than the contents of fluxing elements in the melt and the overall conclusion is that fluorine is less important (relative to melt compositions) than previously thought for the control on the behavior of high field strength elements in highly evolved granitic melts. Moreover, this study confirms that although Nb, Ta, Zr and Hf are all high field strength elements, Nb-Ta and Zr-Hf are complexed differently.

2.2 Introduction

Concentrations of trace elements in granitic melts change significantly as crystallization advances. The main factor that controls whether elements concentrate in the residual melt or disseminate in the major or accessory minerals is the compatibility of those elements between minerals and the melt and the solubilities of accessory minerals. The latter are governed by the change in temperature, pressure and the melt composition. Niobium (Nb), tantalum (Ta), zirconium (Zr) and hafnium (Hf) are high field strength elements (HFSE), and these elements do not substitute into most rock forming-minerals, thus they are concentrated in the silicate melts by fractional crystallization until the saturation of accessory phases such as columbite or zircon is reached.

Generally, rare element pegmatites are the major source for HFSE deposits. Based on their contents of trace elements, rare element pegmatites were classified into two families, LCT (stands for Li, Cs and Ta) and NYF (stand for Na, Y and F) (Cerny and Ercit 2005). These two families known by their peraluminous nature, however, the NYF-family tends toward alkaline composition (London, 2008). Both families are enriched in HFSE and contain elevated amounts of fluxing elements such as H_2O, P, Li, B and F (Linnen and Cuney 2005). Fluxing elements play an important role in magma evolution by causing significant changes in the melt structure which affect melt properties such as viscosity and diffusivity (London, 2008).

There have been many investigations on the solubilities of Nb, Ta, Zr and Hf minerals in granitic melts at different temperatures, pressures and melt compositions (Linnen and Keppler, 1997; Linnen and Keppler, 2002; Bartels et al., 2010; Van Lichtervelde et al., 2010). According to these studies melt composition and temperature (in subaluminus to peraluminous melts) have a greater effect on solubility relative to pressure. Similarly, the melt content of Li, H_2O and P were investigated (Wolf and London, 1993; Linnen, 1998; Linnen, 2005 and Bartels, 2010), however, their effects on solubility are less pronounced comparing to melt composition and temperature.

Fluorine is one of the fluxing elements that usually associated with rare element granites and pegmatites (Linnen, 1998). Thus, understanding the effects of fluxing elements on the behavior of HFSE elements in granitic melts is crucial. However, effect of fluorine on the solubilities of Nb, Ta, Zr and Hf minerals is controversial. Keppler (1993) reported that the solubilities of Nb, Ta and Zr minerals increase with increasing F content in the melt. The enhancement of solubility was explained by increasing NBO in the melts due to the reaction of F with Al to form AlF_6^{-3} complexes. Van Lichtervelde et al. (2010) concluded that F has a weak effect on Mn-tantalite and zircon solubilities. By contrast, Fiege et al (2011) showed that F has no effect on the solubilities of Mn-tantalite and Mn-columbite in subaluminous haplogranitic melts. Moreover, Baker and Conte (2002) reported that adding 0.35 wt. % Cl or 1.2 wt. % F to the melt has a weak effect on both solubility and diffusivity of Zr in nearly water-saturated metaluminous granitic melts at 1,200 to 1,050 °C, and 1 kbar.

The main motivation behind this work is to resolve the controversies surrounding the effect of F on the solubilities of Nb, Ta, Zr and Hf minerals. The effects of fluorine on the solubilities of Nb, Ta, Zr and Hf minerals will be investigated further, as well as temperature and the melt ASI (molar Al/[Na+ K]). This will be accomplished by using a series of haplogranitic glasses that have constant

compositions except for fluorine contents, to study such effects; and an Al-rich haplogranitic glass to examine the F effect at a different melt ASI.

2.3 Methodology

2.3.1 Starting glasses

A highly fluxed synthesized glass (haplogranitic) was prepared by mixing SiO_2, Al_2O_3, Na_2CO_3 and K_2CO_3, and heated gradually to degas the CO_2. The melt corresponds to the intersection of the granite minimum with the albite-orthoclase tieline ($Ab_{72}Or_{28}$) in the quartz-albite-orthoclase system (Q-Ab-Or) due to the addition of P_2O_5 to the melt (London et al, 1993). About 1.1, 1.7 and 2.02 wt. % of Li_2O, P_2O_5 and B_2O_3, respectively were added as Li_3PO_4, and B_2O_3 to the starting mixture to obtain a highly fluxed glass. The mixture was loaded into a platinum crucible and placed in a furnace at 1200 °C for 24 h. After 24 h, the melt was quenched and the glass was crushed and ground into a fine powder in an agate mortar. To insure homogeneity, the glass was reheated and ground a second time. Before grinding, small pieces of the glass were taken to be analyzed by electron microprobe (EMP) then the rest was ground into fine powder, which also was analyzed by ICP-MS.

In order to study the effect of fluorine on the solubility of Mn-columbite, Mn-tantalite, zircon and hafnon, three fluorine-rich glasses were prepared with approximately 2, 4, 6 wt. % F by adding AgF to the initial glass. The molar ASI (Al/[Na+K]) ratio and the molar ASI_{Li} (Al /[Na+K+Li]) are almost constant in all experiments (about 1.05 and 0.85, respectively) and the only variable is the fluorine concentration. A fourth F-rich glass was prepared by adding AlF_3. This glass in nominally peraluminous and has a F content of 6 wt. %. The molar ASI (Al/[Na+K]) ratio and the molar ASI_{Li} (Al/[Na+K+Li]) of peraluminous glass are 1.32 and 1.04, respectively. About 400 mg of the starting glass powder and variable amounts of AgF or AlF_3 were mixed and loaded in gold capsules (3 cm

length and 5mm o.d.) with 8 wt. % (32 mg) H_2O to be nearly water saturated. Capsules were then shut and sealed by arc welder and placed in rapid quench cold seal pressure vessels (CSPV) at 2 kbars and 800 °C for five days. Later, the fluorine-rich water saturated glasses were crushed and ground into fine powder.

2.3.2 Starting minerals

Synthetic Mn-columbite, Mn-tantalite, hafnon and natural zircon (from Miask, Ural) were used to conduct solubility experiments. Theses minerals are commonly associated with evolved granites and pegmatites except for hafnon which is not found in nature. Although pure oxides of these elements (e.g. Nb_2O_5…etc.) can be used to conduct solubility, they were not used because their existence in nature as pure oxides is very rare.

The solubility experiment consists of gently mixing about 30 mg of fluorine-rich glass and 3 mg of crystals of the investigated minerals. The mixture was loaded into a gold capsule (2 cm length and 3 mm o.d.) shut and sealed by an arc welder then placed in drying oven at 110 °C. Before starting the experiments, capsules were weighed to ensure there was no leakage, and then placed in autoclaves at 700 to 1000 °C and 2 kbars for two to five days. After five days, the experiments were quenched isobarically, and then small chips were taken and mounted in an epoxy puck to be analyzed by electron microprobe after polishing.

In order to study the effect of F on the solubilities of Mn-columbite, Mn-tantalite, zircon and hafnon at different ASI, four experiments were conducted at 800 and 2 kbars using AlF_3 as a fluorine source, following the same procedures described above. Four series experiments for each investigated mineral with variable F concentrations were conducted at 1000 °C in order to study the effect of temperature on the solubility and also to perform reverse experiments to approach equilibrium from an over-saturated melt. About 70 mg hydrous glasses and about 7 mg crystals (e.g. Mn-columbite...

etc.) were loaded into platinum capsules, then shut and sealed by an arc welder. All high temperature experiments were conducted in vertically mounted internally-heated pressure vessels (IHPVs) at the University of Hannover, Germany. Experiments were prepared with the same aforementioned procedures, and placed into IHPVs at 1000 °C and 2 kbars for two days. About 50 % of the product of each experiment was used for EMP analysis and the other 50 % was used to conduct the reverse experiments.

Reverse experiments were performed by using the glass products of the high temperature experiments. About 50 mg of glass were loaded into gold capsules and doped with about 3 mg of crystals in an attempt to prevent the nucleation of microcrystals. Capsules were prepared using the procedures described above, then placed in CSPV for five days at 800 °C and 2 kbars. Later, small pieces of glass were taken to be analyzed by EMP.

2.3.3 Analytical techniques

All quenched experiments were weighed before opening to check for leaks. The experimental products were mounted in epoxy then polished. The concentrations of Li and B in the starting material were taken to be the same as the starting glass measured by inductively coupled plasma mass spectroscopy (ICP/MS). The concentration H_2O was estimated from the EMP analysis, but according to Linnen (2005), the effect of water on the solubilities of HFSE minerals is negligible for melts with greater than 3 wt. % H_2O. The major elements (except for Li, B and H_2O) of the starting glass, including their fluorine contents, were analyzed by a JEOL 733 microprobe at CANMET laboratory, Ottawa, Canada. Metal concentrations as well as major elements, were analyzed by a Cameca SX50 electron microprobe at University of Toronto and a Cambax MBX microprobe at Carleton University, Ottawa, Canada. However, the CANMET analysis of major elements analysis is preferred because it shows more reliable comparing to ICP analysis and calculated concentrations.

The concentrations of Na, K, Al, Si, F and P were measured with a 15 kV accelerating voltage, 20 nA beam current, 10 seconds counting time for Al and Si, and 6 seconds for the rest of the elements and the beam diameter was 20 micrometers. The respective standards for the major elements were synthetic NaNb glass for Na, obsidian glass for Al, Si and K, synthetic CaF_2 glass for F and natural apatite for P. Trace element Nb, Ta, Zr and Hf concentrations were measured with 15 kV accelerating voltage, 60 nA beam current, counting time was between 40 and 60 seconds, and the beam diameter was 5 micrometers. The standards for the trace elements analysis were synthetic NaNb glass for Nb, Ta metal for Ta, synthetic $ZrSiO_4$ for Zr and synthetic $HfSiO_4$ for Hf. Oxygen was calculated by cation stoichiometry and included in the matrix correction, and oxygen equivalent from F, was subtracted in the matrix correction. The method of matrix correction was ZAF or Phi-Rho-Z calculations, and the mass absorption coefficients dataset was CITZMU.

The Li and B contents in the starting glass, as well as the contents of the other major, elements were measured by inductively coupled plasma mass spectroscopy (ICP/MS) at ACTLABS facilities. For Li and B, glasses underwent a sodium peroxide fusion, followed by sintered at 650 °C in a muffle furnace and then dissolved in a solution of 5% nitric acid before ICP-MS analysis. The rest of the elements were measured using lithium metaborate/tetraborate fusion-ICP-MS method. In this method, the fused sample is diluted and analyzed by a Perkin Elmer Sciex ELAN 6000, 6100 or 9000 ICP-MS.

2.4 Results

The compositions of the starting glasses are given in Table 2-1. All solubility experiment products were glasses and crystals of investigated minerals and no other phases were observed. Careful analysis was conducted to determine the concentrations of major and trace elements in all glasses. Some major elements such as Na and F are difficult to analyze by EMP because they tend to diffuse

away from the analyzed area during analysis. The starting glasses as well as some of the run glasses were analyzed by EMP at the CANMET laboratory in Ottawa for both major and trace elements. Comparing CANMET results to those obtained by ICP/MS, shows very similar concentrations of major elements (Na in particular) and the F concentrations are similar to values anticipated from glass synthesis. However, the results obtained from EMP at University of Toronto show very low Na and F concentrations, which were attributed to the diffusion problem during analysis, but the trace element concentrations from the University of Toronto analysis are similar to those from CANMET. Therefore, the major element contents in the run glasses are assumed to be the same as their concentration in the starting glasses and they are given in Table 2-1. The concentrations Nb, Ta, Zr, Hf and Mn were analyzed by electron microprobe and the results are given in Tables 2-2, 2-3, 2-4 and 2-5. Generally, the molar ratios of Mn/Nb and Mn/Ta in the glasses are close to the stoichiometric values of Mn-columbite and Mn-tantalite (Table 2-2 and 2-3), which supports the interpretation that these are equilibrium values (Fiege et al., 2011). The dissolution reactions of these experiments have been discussed by Linnen and Keppler (1997), Linnen and Cuney (2005) and Bartels et al. (2010), and they can be written as

$MnNb_2O_6^{crystal} = MnO^{melt} + Nb_2O_5^{melt}$

$MnTa_2O_6^{crystal} = MnO^{melt} + Ta_2O_5^{melt}$

The results of the dissolution reactions can be expressed in terms of solubility products

K_{sp}^{MnNb} (mol^2/kg^2) = X (MnO) (mol/kg) . X (Nb_2O_5) (mol/kg)

K_{sp}^{MnTa} (mol^2/kg^2) = X (MnO) (mol/kg) . X (Ta_2O_5) (mol/kg)

Where X represents the molar concentration of MnO, Nb_2O_5 and Ta_2O_5 in the melt.

Experiments that were carried out at 1000 °C also show stoichiometric values. The results of these experiments show that Mn-tantalite is more soluble than Mn-columbite at the same conditions which are in agreement with Keppler (1993), Linnen and Keppler (1997), Bartels et al. (2010) and

Fiege et al. (2011). The reverse experiments of Mn-columbite (SO.42R) and Mn-tantalite (SO.43R) solubilities at 800 C show nucleation of very small crystals throughout the glass, which might affect EMP analysis. However, clean areas were found around large seed crystals, and these areas were used for EMP analysis (Fig.2-1). One problem is that the average Mn/Nb ratio obtained from experiments conducted at 700 °C is 0.84 which is greater than the stoichiometric value 0.50, whereas Mn/Ta for the 700 °C experiment has an average ratio of 0.28. These nonstoichiometric values could be due to slower diffusivity at lower temperature. However, the values of the solubility products at 700 °C, are consistent with those extrapolated from higher temperatures (see below), therefore, we interpret that these are close to equilibrium solubilities, and at worst represent minimum values.

The dissolution reactions of zircon and hafnon are:

$ZrSiO_4^{crystal} = ZrO_2^{melt} + SiO_2^{melt}$

$HfSiO_4^{crystal} = HfO_2^{melt} + SiO_2^{melt}$

The equilibrium constant of zircon and hafnon dissolution reaction can be written as

$K_{ZrSiO4} = (a_{ZrO2}^{melt}.\ a_{SiO2}^{melt}) /\ a_{ZrSiO4}^{crystal}$

$K_{HfSiO4} = (a_{HfO2}^{melt}.\ a_{SiO2}^{melt}) / a_{HfSiO4}^{crystal}$

where α is the activities of $ZrSiO_4$, $HfSiO_4$, ZrO_2, HfO_2 and SiO_2. However, the activities of $ZrSiO_4$ and $HfSiO_4$ are equal to 1 because pure zircon and synthetic hafnon were used in these experiments. Therefore;

$K_{ZrSiO4} = a_{ZrO2}^{melt}.\ a_{SiO2}^{melt}$

$K_{HfSiO4} = a_{HfO2}^{melt}.\ a_{SiO2}^{melt}$

The activity of silica in the melt is changed by the addition of fluxing compounds as evidenced by the shift of the granite minimum composition away from the SiO_2 apex. However, given the total amount of fluxes in this study, and that an insignificant amount of SiO_2 was added to the melt by the

dissolution of zircon and hafnon, a_{SiO2}^{melt} was assumed to be nearly constant. Consequently, the solubility of zircon and hafnon are reported as wt.% and mol/kg dissolved into the melt (Table 2-4 and 2-5). Glass, zircon and hafnon crystals were the only phases observed in most experiments. However, backscattered images show some hafnon crystals have a light gray phase in their cores. Microprobe analysis of these phases showed that they consist of about 90 wt. % HfO_2 and 9.18 wt. % SiO_2, which indicates unreacted HfO_2 from the hafnon synthesis experiments. The same problem was reported by Linnen (1998) and was explained by unreacted or excess HfO_2. These are always in crystal cores, and generally are rare, and thus they do not affect hafnon solubility.

2.4.1 Temperature dependence

The temperature dependence of the logarithmic values of Mn-columbite and Mn-tantalite solubility products is shown in figures 2-2 and 2-3. The solubility products show linear relationships with temperature (1000/K). The solubilities products of Mn-columbite and Mn-tantalite increase from -3.24 ± 0.02 (mol^2/kg^2), -2.75 ± 0.02 (mol^2/kg^2), respectively, at 700 °C, to -1.77± 0.01 and -1.76 ± 0.02, respectively, at 1000 °C. The solubility values of Mn-columbite and Mn-tantalite at 600 °C (-4.0 and -3.2(mol^2/kg^2), respectively) were extrapolated from the equation of the regression lines in figures 2-2 and 2-3. The data of Linnen and Keppler (1997) and Fiege et al. (2011) were reported for comparison. The solubility products of Mn-columbite and Mn-tantalite of the experiments conducted at 700 °C, are plotted with the data from experiments conducted at 800 and 1000 °C, and the linear regressions of two series of experiments have R^2 values of 0.99 and 0.97, respectively. If only the data for 1000 and 800 °C are used, the values extrapolated to 700 °C are close to the 700 °C data obtained from dissolution experiments (Figs.2-2 and 2-3), which indicate that the data from 700 °C are close to equilibrium.

2.4.2 Fluorine dependence

2.4.2.1 Mn-columbite and Mn-tantalite

The solubility products of Mn-columbite and Mn-tantalite are plotted against fluorine concentration in the melt (Figs. 2-4 and 2-5). The results show that F has no effect on the solubilities of Mn-columbite and Mn-tantalite at least at the experimental conditions and the investigated composition, which is in agreement with Fiege et al (2011). This contradicts the results of Keppler (1993), who reported that F increases the solubilities of Mn-columbite and Mn-tantalite. According to Fiege et al (2011) the difference may be due to difficulties of reaching equilibrium in the experiments that were conducted at low temperature. At equilibrium, the Mn/Nb and Mn/Ta ratios in the melt should be around 0.50. However, Keppler's (1993) experiments conducted at 800 °C and 2 kbars show values larger than 0.50. Another possible reason is related to the melt composition that has been used in this study which contains Li and it may behave like an alkali as well as a flux (Van Lichtervelde et al., 2010). Alkalis in silicate melts modify the silicate structure by breaking up the network between Si-tetrahedra, and provide melts with more NBO (Linnen and Keppler, 1997). Also Nb and Ta and other M^{5+} cations have strong affinity with Al in peraluminous melts (Horng et al., 1999) which may form a simpsonite-type complex (Al-TaO (OH)) in peraluminous melts (Van Lichtervelde et al 2010). Therefore, it is better to say that F has no effect on Mn-columbite and Mn-tantalite solubilities at this work experimental conditions.

2.4.2.2 Zircon and hafnon

The solubilities of zircon and hafnon are plotted against F concentration in the melt in figure 2-6. Watson (1979) reported that the solubility of zircon in water saturated haplogranitic melts (ASI=1.0) at 800 °C and 2 kbars is less than 100 ppm of Zr. This work data show dramatic increases in the solubilities of zircon and hafnon from 0.25 ± 0.04 and 0.85 ± 0.05 wt. %, to 0.47 ± 0.03 and

1.30 ± 0.09 wt. %, respectively, with increasing F concentration from 0 to 8 wt. %. These results are in agreement with Keppler (1993) where similar behavior of Zr was reported, which was interpreted as possible direct reaction between F and Zr or due to the NBO generated by the existence of F in the melt which could form complexes with Zr. However, the saturation level of zircon in this study is much higher than Keppler (1993), which could be due to the more alkaline nature of glasses in this study.

2.4.3 Attainment of equilibrium

In order to demonstrate equilibrium, the experiment duration should be long enough to reach equilibrium and the Mn/Nb and Mn/ Ta ratios must be constant throughout the melt at experimental conditions (tables 2-2 and 2-3). Based on the previous work (e.g. Linnen and Keppler (1997), Bartels et al. (2010) and Fiege et al. (2011)), experiments duration between four to eight days should be sufficient to reach equilibrium. The melts in this study are flux rich and slightly more alkaline than those of Fiege et al (2011) Therefore, the diffusivities of Nb, Ta, Zr, Hf and Mn are faster than the diffusivities of the same elements in peraluminous melts or flux free melts. Thus, experiments with five days duration should be long enough to reach equilibrium.

Equilibrium is best demonstrated if the values for dissolution and crystallization experiments are the same. Two glasses (0 wt. % F and 6 wt. % F) were chosen to conduct reverse experiments at 800 °C and 2 kbars. The results of these experiments (crystallization experiments) show that the solubility values are close to those obtained from dissolution experiments, which indicates that five days is enough to reach equilibrium (Figs. 2-4, and 2-5).

2.5 Discussion

2.5.1 Composition dependence and the effect of fluxing elements

2.5.1.1 Mn-columbite and Mn-tantalite

The solubility products of Mn-columbite and Mn-tantalite in F free glasses (ASI 1.05) were plotted against the molar of Al-Na-K per kilogram (reported as ASI^{+} in the tables), and compared to previous studies (Figs. 2-7a and 2-8a). This comparison shows that this work data has higher solubility than Linnen and Keppler (1997) at equivalent melt compositions. Similarly, Linnen (1998), Bartels et al. (2010) and Van Lichtervelde et al. (for Ta, 2010) reported higher solubilities than Linnen and Keppler (1997), whereas Fiege et al. (2011) data are very close to Linnen and Keppler (1997). These high solubility values reported in this study, Linnen (1998), Bartels et al. (2010) and Van Lichtervelde et al. (2010), appear to be due to the high concentrations of fluxing components in the melts.

The presence of Li^{+} and Mn^{2+} in silicate melt breaks bridging oxygen (BO) between silicon tetrahedra. The addition of Li^{+} may generate one non-bridging oxygen (NBO, i.e. oxygen ions that are not shared by two tetrahedra) and divalent ions such as Mn^{2+} generate two NBO (Linnen and Keppler, 1997). Thus the melt composition term was modified to include Li and Mn as network modifiers. In figures 2-7b and 2-8b, K_{Sp}^{MnNb} and K_{sp}^{MnTa} were plotted against the molar of Al-Na-K-Li-2Mn per kilogram (reported as ASI^{+}_{Li} in the tables). On these figures, the solubility values of this work (ASI 1.05), Bartels et al. (2010) are lower than those from Linnen and Keppler (1997), whereas Linnen (1998) and Van Lichtervelde et al. (2010) data points are close or fit the Linnen and Keppler (1997) curve (Van Lichtervelde at al., 2010 is only for Ta). Therefore, the last two data points of Linnen (1998) and Van Lichtervelde et al. (2010), that fit Linnen Keppler curve (1997), support Linnen (1998) approach that solubilities of Mn-columbite and Mn-tantalite increase with increasing Li

concentration in the melt. However, all data that are below the reference curve contain P and B, which could decrease the Mn-columbite and Mn-tantalite solubilities.

The presence of P and B in the melts plays important roles in the silicate melt properties (e.g. lower the solidus temperature and reduce the viscosity of the melts, London, 1987); however, their effects on the solubilities of Mn-columbite and Mn-tantalite are still not clear. Peraluminous data of Wolf and London (1993) showed that B has no effect on the solubilities of Mn-columbite and Mn-tantalite, whereas P increases the solubility. In more general terms, Toplis and Dingwell (1996) reported that the additional of P_2O_5 in peralkaline melts shifts the effective ASI to be more peraluminous by reacting with alkalis through the reaction

2 Si–O– M + P–O–P = 2 P–O–M + Si–O–Si

where M is a network modifier (i.e. breaks up the bonds between silicon tetrahedra) cation such as Na^+ or K^+. The additional of P decreases the number of network modifiers, which decreases the number of NBO and it can be predicted that the solubilities of Mn-columbite and Mn-tantalite should decrease. Therefore, P was included in the melt composition term as the molar Al-P-Na-K-Li-2Mn per kilogram was plotted against K_{Sp}^{MnNb} and K_{sp}^{MnTa} (Figs. 2-7c and 2-8c). The comparison shows that most of the data are close or fit the reference curve of Linnen and Keppler (1997), i.e. that P apparently decreases the solubilities of Mn-columbite and Mn-Tantalite by shifting peralkaline melts toward subaluminous compositions.

Figures 2-7 and 2-8 also show K_{Sp}^{MnNb} and K_{sp}^{MnTa} values in peraluminous melt (ASI 1.32). In peraluminous melt, the Mn-tantalite is more soluble than Mn-columbite. Similar behavior was reported by Linnen and Keppler (1997), which was explained by the differences in the chemical bonding around Nb^+ and Ta^+ in subaluminous melts. Another observation is that the values of Mn-columbite and Mn-tantalite solubilities are higher than those from Linnen and Keppler (1997). That

could be attributed to the presence of P in the peraluminous melt. In peraluminous melts, the effect of P on the silicate structure still not clear. Two mechanisms were proposed for the way that P reacts with peraluminous melts structure (Toplis and Dingwell, 1996). The first mechanism suggests the reaction of P_2O_5 with tetrahedral Al:

$2SiAlO_2 + P_2O_5 = 2AlPO_4 + Si\text{-}O\text{-}Si$

The second mechanism is that P_2O_5 reacts with Al that exists as a network modifier:

$Al_2O_3 + P_2O_5 = 2AlPO_4$

However, Gan and Hess (1992) reported an increase of Raman bands associated with Si-O-Si vibrations which supports the first mechanism. In order to test P effect, the ASI was modified to take in account the P effect on the solubility in subaluminous melt, and was given the name effective ASI (ASI_{eff}^{+}) which defines as the molar of Al+P-Na-K-Li-2Mn per kilogram (reported as ASI_{eff}^{+} in the tables). The effective ASI was plotted against solubility products of Mn-columbite and Mn-tantalite (Figs. 2-7c and 2-8c). The values of this study are very close to Linnen and Keppler (1997) curve, which means that P affects the solubilities of Mn-columbite and Mn-tantalite in subaluminous melts. However, since the melts used in this and previous studies have multiple fluxes, the effect of P cannot be measured precisely. Therefore, further systematic studies focusing on P effects on the solubilities of Mn-columbite and Mn-tantalite at different ASI are needed.

2.5.1.2 Zircon and hafnon

In order to investigate whether the fluxed elements in the melt have an effect on zircon and hafnon solubilities, the results of F-free experiments of this study were plotted against molar Al-Na-K per kilogram, and compared to fluxed free glasses of Watson (1979) and Linnen and Keppler (2002), as well as the study of Linnen (for hafnon, 1998) in Li-free to Li-rich glasses (Figs. 2-9a and 2-10a). The results of this study are higher than those of Watson (1979) and Linnen and Keppler (2002) (Fig.

2-9a), and also higher than Linnen (1998) for the glass that contains 1 wt. % Li_2O (Fig. 2-10a) at equivalent molar Al-Na-K per kilogram . Again these higher values could be related to the fluxing contents in these melts. Therefore, the solubilities of Zr and Hf were plotted against molar Al-Na-K-Li-2Mn per kilogram (Figs. 2-9b and 2-10b). Using this melt composition parameter, zircon and hafnon solubilities are below the curve of Watson (1979) and Linnen and Keppler (2002), which suggests that either Li is not acting as a network modifier or the presence of Li in the melt decreases the solubilities of Zr and Hf. Linnen (1998) reported that the increase of Li_2O concentration in the melt decrease the solubilities of Zr and Hf, and proposed that the strong bond formed between Li and oxygen due to the small ionic radius of Li compared to the larger ionic radius of Na or K. Thus, the competition between Zr^{4+} and Hf^{4+} on the NBO that bonds with Li is more difficult, whereas it is easier in the case of Nb^{5+} and Ta^{5+} due to the high charge and smaller ionic radius.

The effect of P on the solubilities of zircon and hafnon is shown in figures 2-9c and 2-10c. The solubilities were plotted against the molar Al-P-Na-K-Li per kilogram. The comparison shows that both zircon and hafnon solubilities are close to the reference curve of Watson (1979), which support the positive effect of P on the solubilities of zircon and hafnon. However, the roles of fluxed elements in silicate melts need further individual investigation for each element.

In peraluminous melts, the data shows that hafnon is less soluble than in peraluminous melts. However, this study's results show that hafnon solubility is higher than the solubility obtained by Linnen (1998) at ASI_{Li} = 1.04, even with the negative effect of Li on hafnon solubility (Fig. 2-10). This high value can be attributed to the presence of about 4 wt. % F. However, it is difficult to interpret the effect of Li and other flux components because of the complex composition of the peraluminous melt and the variation of the fluxed contents between glasses of this study and the glasses of the previous studies.

2.5.1.3 The role of fluorine in the melt

Fluorine, as other fluxes (H_2O, B, P), has a significant role in silicate melts. The presence of F in silicate melts reduces the viscosity and increases the diffusion coefficient (Dingwell et al., 1985) due to the depolymerization effect of F on silicate melts. Schaller et al. (1991) reported that F preferentially coordinates with Al to form octahedral AlF_3 in anhydrous nephleline, jadeite and albite glasses. The presence of F-Si and F-alkalis was reported to be unlikely based on cross-polarization / magic angle spinning (CP/MAS) and nuclear magnetic resonance (NMR) spectra. The decrease in viscosity with increasing F content in the melt was explained by the complexing F with Al from bridging AlO_4, which causes depolymerization of the melts. This process will increase the amount of NBO which will increase the solubilities of HFSE in the melts. Keppler (1993) showed that increasing F content in the water-saturated haplogranitic melt increases the solubility of Mn-columbite, Mn-tantalite, rutile and zircon at 800 C° and 2 kbars. The mechanism that was proposed is that F could react directly with HFSE and form fluorocomplexes, or could react with NBO generated by the reaction of F with bridging AlO_4.

Based on the results from this study, no change in Mn-columbite and Mn-tantalite solubilities was observed with increasing F content in the melts. That could mean that F does not react with bridging Al to generate NBO, nor reacts with Nb and Ta. By contrast, a linear trend was observed in zircon and hafnon with increasing F content in the melt. Another possible coordination of F in the silicate melts is by reacting with alkalis or Si. If F reacts with alkalis, that would decrease the solubility of Mn-columbite and Mn-tantalite. From this study, a slight decrease in solubility was observed in both Mn-columbite and Mn-tantalite experiments, which could mean that a small amount of alkalis reacts with F. However, according to Schaller et al., (1991) F-alkalis spectra was not found in his study.

By contrast, zircon and hafnon solubility increase significantly with increasing F content in the melt. This could support an argument that F reacts with Al-Si to produce AlF_3, and hence increase NBO. However, this hypothesis was rejected because if true, the solubilities of Mn-columbite and Mn-tantalite should increase with increasing F, but that was not observed. Consequently, since the only difference between these experiments is the minerals that dissolve, the increase in zircon and hafnon solubilities could be due to the direct reaction between F and Zr or Hf, but not Nb and Ta, in the melt (Keppler, 1993). However, Farges (1996) showed that F was not found as first neighbors around Zr in F-bearing albitic glass. Therefore, more analysis (X-ray absorption fine structure (XAFS) and NMR) on the melt structure are needed to show the effect of F on the solubilities of HFSE minerals and support the hypothesis of the direct coordination of F with Zr and Hf, but not Nb and Ta, in the investigated melts.

2.6 Conclusions and implications for natural systems

This study shows that solubilities of Mn-columbite and Mn-tantalite are nearly independent of the F content of the melt, approximately 18.19 ± 1.2 and 43.65 ± 2.5 $x10^{-4}$ K_{SP} (mol^2/kg^2), respectively, in a highly fluxed water-saturated haplogranitic melt at 800 °C and 2 kbars. By contrast, the solubilities of zircon and hafnon increase from 2.03 ± 0.03 $x10^{-4}$ (mol/kg) ZrO_2 and 4.04 ± 0.2 $x10^{-4}$ (mol/kg) HfO_2 for melts with 0 wt. % F to 3.81 ± 0.3 $x10^{-4}$ (mol/kg) ZrO_2 and 6.18 ± 0.04 $x10^{-4}$ (mol/kg) HfO_2 for melts with 8 wt. % F.

The results of this study indicate that melt ASI has a greater effect on the solubilities of investigated minerals than the concentrations of fluxing components in the melt. The results of this study confirms that Mn-tantalite is more soluble than Mn-columbite, particularly for the subaluminous melt composition (ASI_{Li} = 1.04).

The comparison of this study data with previous studies data shows that fluxing elements have variable effects on the solubilities of Mn-columbite, Mn-tantalite, zircon and hafnon. The presence of Li in the melt appears to increase the solubilities of Mn-columbite and Mn-tantalite, whereas Li decrease the solubilities of zircon and hafnon, in support of Linnen (1998).

The roles of P and B in the silicate melt and their effects on the solubilities of investigated minerals are not clear. However, the solubility data imply that P decreases the solubilities of all investigated minerals in peralkaline melt (ASI_{Li} = 0.85) by reacting with alkalis in the melt structure, which decreases NBO. It is difficult to predict the role of P in subaluminous melts. In subaluminous melts P could react with either alkalis and form P-O-M complexes (M are alkali cations), or with Al to form $AlPO_4$ complexes (Toplis and Dingwell, 1996).

Generally, the effect of fluxing elements on the solubilities of Mn-columbite, Mn-tantalite, zircon and hafnon is poorly understood. The variable effects of fluxing elements on the solubilities make the comparisons of the results of this study and the results of the previous studies very difficult especially in peraluminous melts where the melt become more complex. Therefore, further investigations on the roles of Li, P and B in silicate melts are needed to understand their effects on the solubilities of HFSE, which requires systematic experiments to be conducted for each element in peralkaline, subaluminous and peraluminous, melt compositions.

In order to show the implication of this work for natural systems, the results must be extrapolated to temperatures at which pegmatites start crystallizing. Usually, pegmatites crystalize at temperatures around 600 °C (Cerny, 2005 and Linnen and Cuney, 2005); hence K_{Sp}^{MnNb} and K_{sp}^{MnTa} were extrapolated to 600 °C. The extrapolated data for solubility products K_{Sp}^{MnNb} and K_{sp}^{MnTa} at 600 °C are 0.97 and 2.23(mol^2/kg^2).10^{-4}, respectively. Linnen (1998) suggested that 500 ppm MnO is representative for a composition of a rare element pegmatite melt. Therefore, in a melt that contains 1

wt. % Li_2O and which has an ASI = 1.05 (or ASI_{Li} = 0.85), the amounts of Nb and Ta required to precipitate Mn-columbite and Mn-tantalite are 2553 and 9700 ppm, respectively. However, in flux free melts only 70 ppm Nb and 510 ppm Ta are required to crystallize Mn-columbite and Mn-tantalite (Linnen and Keppler, 1997). Thus, once Li content in the melt starts to decrease by crystalizing Li minerals (e.g. spodumene) the solubilities of Mn-columbite and Mn-tantalite decrease and they may start to crystallized. Similarly, a decrease in alkali contents or increase in Al content in the melt decreases the solubilities of Mn-columbite and Mn-tantalite. However, Ta mineralization is not associated with Li minerals in same zone, e.g. Tanco (Cerny, 2005), thus it is more likely that an increase in Al/alkalis ratio is responsible for the reduction in Mn-columbite and Mn-tantalite solubilities. There are two models that have been proposed to explain this separation of Li and Ta mineralization, (1) boundary layer effect during rapid cooling (London, 1999), and (2) the coexistence of at least two immiscible melts in pegmatite formation (Thomas et al., 2006b). In the first model, a boundary layer enriched in H_2O, F, B and incompatible elements, builds up at the crystal-front by segregation of the elements that are not incorporated in the crystallized phase. The second model suggested the formation of two melts, one a peraluminous melt (type A), and the other is a water-rich peralkaline melt (type B) (Thomas et al., 2006b; 2009). The model suggested that these two distinct melts are generated from a single homogenous melt which become no longer stable at low pressure (about 1 kbar), and then separates into two melts.

Zr and Hf mineralization are commonly associated with Nb and Ta mineralization. However, this study shows that some factors that affect zircon and hafnon solubilities (Li and F contents in the melt) do not have the same effects on Mn-columbite and Mn-tantalite. The presence of F in the melt increases the solubilities of zircon and hafnon, whereas Li decrease the solubilities of zircon and hafnon and increase the solubilities of Mn-columbite and Mn-tantalite. However, the factor that has

the same effect on the solubilities of columbite-tantalite and zircon-hafnon is the melt ASI. Decreasing the alkalis content or increasing the Al content in the melt leads to a decrease in the solubilities of all investigated minerals. Van Lichtervelde (2007) showed that zircon associated with Ta mineralization and some zircon crystals contain inclusions of Ta oxides, and that shows that zircon and Ta oxide crystallized from the same melt at the same time. Therefore, similar processes that lead to Nb and Ta crystallization could be also responsible for zircon and hafnon saturation. Thus, it is possible that either boundary layer or the presence of more than immiscible silicate melts is in control of zircon and hafnon saturations. However, the boundary layer model is more plausible because it can explain the separation of HFSE (incompatible) from alkalis, by partitioning away from the crystal boundary.

2.7 Future work

The effects of F on the solubilities of Nb, Ta, Zr and Hf minerals were investigated in this study and it was shown that F has a variable effect on HFSE minerals solubilities at constant ASI, flux contents and pressure. In order to fully understand F effect on the solubility, further experiments at variable ASI (peralkaline to peraluminous) are needed. Moreover, the actual F coordination in the melt is poorly understood. Previous work suggested a direct reaction between F and HFSE to explain the increase in solubility (Keppler, 1993). Keppler, (1993), Schaller et al. (1991) and Farges, (1996) suggested that the increase of NBO could explain the enhanced solubility. However, the latter suggestion not believed because an increase in the number of NBO should increase the solubilities of all HFSE minerals, which was not observed in this study. More analysis of glass structures (e.g., XAFS) is needed to understand the actual role of F in silicate melts.

This work can be extended further by studying the effects of the other flux elements, namely Li, P and B, on the solubility of HFSE. These elements must be investigated individually by varying their concentrations in the melt. Moreover, similar experiments at different ASI are suggested to show if these elements behave differently at different ASI.

References

Agangi, A., Kamenetsky, V. S., & McPhie, J. (2010). The role of fluorine in the concentration and transport of lithophile trace elements in felsic magmas: Insights from the gawler range volcanics, south australia. Chemical Geology, 273(3-4), 314-325.

Agulyansky, A. (2004). Synthesis of tantalum and niobium fluoride compounds. Chemistry of tantalum and niobium fluoride compounds (pp. 1-5). Amsterdam: Elsevier Science.

Baker, D. R., Conte, A. M., Freda, C., & Ottolini, L. (2002). The effect of halogens on Zr diffusion and zircon dissolution in hydrous metaluminous granitic melts. Contributions to Mineralogy and Petrology, 142(6), 666-678.

Bartels, A., Holtz, F., & Linnen, R. L. (2010). Solubility of manganotantalite and manganocolumbite in pegmatitic melts. American Mineralogist, 95(4), 537-544.

Bau, M. (1996). Controls on the fractionation of isovalent trace elements in magmatic and aqueous systems; evidence from Y/Ho, Zr/Hf, and lanthanide tetrad effect. Contributions to Mineralogy and Petrology, 123(3), 323-333.

Beus, A. A. (1962). Okolorudnye izmeneniya gidrotermalno-pnevmatoliticheskikh mestorozhdenii redkikh elementov. Sovetskaya Geologiya, 4, 114-126.

Cerny, P. (1991). Rare-element granitic pegmatites. part 1: Anatomy and internal evolution of pegmatite deposits. Geoscience Canada, 18(2), 49-67.

Cerny, P., & Ercit, T. S. (2005). The classification of granitic pegmatites. Mineralogical Association of Canada; 1955-2005, 12.

Cerny, P., Meintzer, R. E., & Anderson, A. J. (1985). Extreme fractionation in rare-element granitic pegmatites; selected examples of data and mechanisms. The Canadian Mineralogist, 23, Part 3, 381-421.

Chappell, B. W., & White, A. J. R. (1992). I- and S-type granites in the lachlan fold belt. Special Paper - Geological Society of America, 272, 1-26.

Collins, W. J., Beams, S. D., White, A. J. R., & Chappell, B. W. (1982). Nature and origin of A-type granites with particular reference to southeastern Australia. Contributions to Mineralogy and Petrology, 80(2), 189-200.

David, K., Schiano, P., & Allegre, C. J. (2000). Assessment of the Zr/Hf fractionation in oceanic basalts and continental materials during petrogenetic processes. Earth and Planetary Science Letters, 178(3-4), 285-301.

Dingwell, D. B., Keppler, H., Knoeller, W., Merwin, L., Schaller, T., & Sebald, A. (1991). A multinuclear NMR study of fluorine in silicate glasses. Program with Abstracts - Geological Association of Canada; Mineralogical Association of Canada; Canadian Geophysical Union, Joint Annual Meeting, 16, 31.

Dingwell, D. B., Scarfe, C. M., & Cronin, D. J. (1985). The effect of fluorine on viscosities in the system Na_2O - Al_2O_3 - SiO_2; implications for phonolites, trachytes and rhyolites. American Mineralogist, 70(1-2), 80-87.

Dolejs, D., & Baker, D. R. (2004). Thermodynamic analysis of the system Na_2O- K_2O- CaO_2-Al_2O_3-SiO_2-H_2O-F_2O^{-1}; stability of fluorine-bearing minerals in felsic igneous suites. Contributions to Mineralogy and Petrology, 146(6), 762-778.

Dolejs, D., & Baker, D. R. (2006). Phase transitions and volumetric properties of cryolite, Na_3AlF_6; differential thermal analysis to 100 MPa. American Mineralogist, 91(1), 97-103.

Dupuy, C., Liotard, J. M., & Dostal, J. (1992). Zr/Hf fractionation in intraplate basaltic rocks; carbonate metasomatism in the mantle source. Geochimica Et Cosmochimica Acta, 56(6), 2417-2423.

Ellison, A. J., & Hess, P. C. (1986). Solution behavior of 4^{+} cations in high silica melts; petrologic and geochemical implications. Contributions to Mineralogy and Petrology, 94(3), 343-351.

Farges, F. (1996). Does Zr-F "complexation" occur in magmas? Chemical Geology, 127(4), 253-268.

Fiege, A., Kirchner, C., Holtz, F., Linnen, R. L., & Dziony, W. (2011). Influence of fluorine on the solubility of manganotantalite ($MnTa_2O_6$) and manganocolumbite ($MnNb_2O_6$) in granitic melts; an experimental study. Lithos (Oslo), 122(3-4), 165-174.

Gan, H., & Hess, P. C. (1992). Phosphate speciation in potassium aluminosilicate glasses. American Mineralogist, 77(5-6), 495-506.

Hildreth, W. (1979). The bishop tuff; evidence for the origin of compositional zonation in silicic magma chambers. Special Paper - Geological Society of America, (180), 43-75.

Hildreth, W. (1981). Gradients in silicic magma chambers: Implications for lithospheric magmatism. Journal of Geophysical Research, 86, 10153-92.

Hill, E., Blundy, J. D., & Wood, B. J. (2011). Clinopyroxene melt trace element partitioning and the development of a predictive model for HFSE and Sc. Contributions to Mineralogy and Petrology, 161(3), 423-438.

Hofmann, A. W. (1988). Chemical differentiation of the earth: The relationship between mantle, continental crust, and oceanic crust. Isotope Studies on the Development of Continental Crust and Mantle, , 90(3) 297-314.

Horng, W., Hess, P. C., & Gan, H. (1999). The interactions between M^{+5} cations (Nb^{+5}, Ta^{+5}, or P^{+5}) and anhydrous haplogranite melts. Geochimica Et Cosmochimica Acta, 63(16), 2419-2428.

Hui, H., Niu, Y., Zhidan, Z., Huixin, H., & Dicheng, Z. (2011). On the enigma of Nb-Ta and Zr-Hf fractionation-A critical review. Journal of Earth Science, 22(1), 52-66.

Kelly, E. D., Carlson, W. D., & Connelly, J. N. (2011). Implications of garnet resorption for the Lu-Hf garnet geochronometer; an example from the contact aureole of the makhavinekh lake pluton, Labrador. Journal of Metamorphic Geology, 29(8), 901-916.

Keppler, H. (1993). Influence of fluorine on the enrichment of high field strength trace elements in granitic rocks. Contributions to Mineralogy and Petrology, 114(4), 479-488.

Keppler, H. (1996). Constraints from partitioning experiments on the composition of subduction-zone fluids. Nature, 380(6571), 237-237.

Kovalenko, V. I., & Kovalenko, N. I. (1984). Problems of the origin, ore-bearing and evolution of rare-metal granitoids. Physics of the Earth and Planetary Interiors, 35(1-3), 51-62.

Linnen, R. L, Samson, I. M. S., & Williams-Jones, A. E. and R., (in press). Geochemistry of rare-metals (Ta-Na-REE-Sn-W) deposits. In S.D. Scott ed., Treatise on geochemistry.

Linnen, R. L., & Keppler, H. (1997). Columbite solubility in granitic melts; consequences for the enrichment and fractionation of Nb and Ta in the earth's crust. Contributions to Mineralogy and Petrology, 128(2-3), 213-227.

Linnen, R. L. (1998). The solubility of Nb-Ta-Zr-Hf-W in granitic melts with Li and Li + F; constraints for mineralization in rare metal granites and pegmatites. Economic Geology and the Bulletin of the Society of Economic Geologists, 93(7), 1013-1025.

Linnen, R. L. (2005). The effect of water on accessory phase solubility in subaluminous and peralkaline granitic melts. Lithos, 80(1-4), 267-280.

Linnen, R. L., & Cuney, M. (2005). Granite-related rare-element deposits and experimental constraints on Ta-Nb-W-Sn-Zr-Hf mineralization. Short Course Notes - Geological Association of Canada, 17, 45-68.

Linnen, R. L., & Keppler, H. (2002). Melt composition control of Zr/Hf fractionation in magmatic processes. Geochimica Et Cosmochimica Acta, 66(18), 3293-3301.

London, D., Morgan VI G., Babb H., Loomis J. (1993). Behavior and effects of phosphorus in the system Na_2O-K_2O-Al_2O_3-SiO_2-P_2O_5-H_2O at 200 MPa (H_2O). Contributions to Mineralogy and Petrology, 113, 450-465.

London, D. (1999). Melt boundary layers and the growth of pegmatitic textures. The Canadian Mineralogist, 37, Part 3, 826-827.

London, D. (2008). Pegmatites. [Quebéc]: Mineralogical Association of Canada.

Marr, R. A., Baker, D. R., & Williams-Jones, A. (1998). Chemical controls on the solubility of Zr-bearing phases in simplified peralkaline melts and application to the strange lake intrusion, Québec - Labrador. Canadian Mineralogist, 36(4), 1001-1008.

Palme, H., & O'Neill, H. S. C. (2004). Cosmochemical estimates of mantle composition. The Mantle and Core, 2 1-38.

Pan, Y., & Bau, M. (1997). Controls on the fractionation of isovalent trace elements in magmatic and aqueous systems; evidence from Y/Ho, Zr/Hf, and lanthanide tetrad effect; discussion and reply. Contributions to Mineralogy and Petrology, 128(4), 405-408.

Pfander, J. A., Jung, S., Munker, C., Stracke, A., & Mezger, K. (2012). A possible high Nb/Ta reservoir in the continental lithospheric mantle and consequences on the global Nb budget - evidence from continental basalts from central Germany. Geochimica Et Cosmochimica Acta, 77, 232-251.

Rudnick, R. L., Barth, M., Horn, I., & McDonough, W. F. (2000). Rutile-bearing refractory eclogites; missing link between continents and depleted mantle. Science, 287(5451), 278-281.

Rudnick, R. L., & Gao, S. (2004). Composition of the continental crust. The Crust, 3 1-64.

Shannon, R. D. (1976). Revised effective ionic radii and systematic studies of interatomic distances in halides and chalcogenides. Acta Crystallographica, Section A (Crystal Physics, Diffraction, Theoretical and General Crystallography), A32, 751-67.

Thomas, R., Webster, J. D., Rhede, D., Seifert, W., Rickers, K., Forster, H. J., Davidson, P. (2006). The transition from peraluminous to peralkaline granitic melts; evidence from melt inclusions and accessory minerals. Lithos, 91(1-4), 137-149.

Thomas, R., Davidson, P., Rhede, D., & Leh, M. (2009). The miarolitic pegmatites from the konigshain; a contribution to understanding the genesis of pegmatites. Contributions to Mineralogy and Petrology, 157(4), 505-523.

Toplis, M. J., & Dingwell, D. B. (1996). The variable influence of P_2O_5 on the viscosity of melts of differing alkali/aluminium ratio; implications for the structural role of phosphorus in silicate melts. Geochimica Et Cosmochimica Acta, 60(21), 4107-4121.

Van Lichtervelde, M., Holtz, F., & Hanchar, J. M. (2010). Solubility of manganotantalite, zircon and hafnon in highly fluxed peralkaline to peraluminous pegmatitic melts. Contributions to Mineralogy and Petrology, 160(1), 17-32.

Van Lichtervelde, M., Salvi, S., Beziat, D., & Linnen, R. L. (2007). Textural features and chemical evolution in tantalum oxides; magmatic versus hydrothermal origins for ta mineralization in the Tanco lower pegmatite, Manitoba, Canada. Economic Geology and the Bulletin of the Society of Economic Geologists, 102(2), 257-276.

Watson, E. B. (1979). Zircon saturation in felsic liquids; experimental results and applications to trace element geochemistry. Contributions to Mineralogy and Petrology, 70(4), 407-419.

Webster, J. D., Thomas, R., Rhede, D., Förster, H., & Seltmann, R. (1997). Melt inclusions in quartz from an evolved peraluminous pegmatite: Geochemical evidence for strong tin enrichment in

fluorine-rich and phosphorus-rich residual liquids. Geochimica Et Cosmochimica Acta, 61(13), 2589-2604.

Wolf, M. B., & London, D. (1993). Preliminary results of HFS and RE element solubility experiments in "granites" as a function of B and P. EOS, Transactions, American Geophysical Union, 74(16), 343.

Yurong, W., Jiatian, L., Jialan, L., & Wenling, F. (1982). Geochemical mechanism of Nb-, Ta-mineralization during the late stage of granite crystallization. Geochemistry (English Language Edition), 1(2), 175-185.

Tables and Figures

Table 1-1 Chemical properties

Elements	Ionic radius* (Å)	Charge	Atomic number	Atomic mass	Ionization energy (kJ/mol)
Nb	0.78	5+	42	92.91	652.1
Ta	0.78	5+	73	180.95	761
Zr	0.86	4+	40	91.22	640.1
Hf	0.85	4+	72	178.49	658.5

* Ionic radius for six-fold coordination number (Shannon, 1976).

Table 2-1 Starting glasses compositions

	D.gls	0.gls	2-gls	4-gls	6-gls	8-gls	gls*
SiO_2	64.01	57.50 (0.95)	56.17 (0.71)	54.7 (0.50)	53.61 (0.36)	51.20 (0.27)	52.82 (0.45)
Al_2O_3	18.73	17.14 (0.29)	16.73 (0.18)	16.3 (0.26)	15.96 (0.13)	15.14 (0.12)	18.83 (0.15)
Na_2O	7.76	7.26 (0.33)	7.06 (0.20)	7.0 (0.10)	6.37 (0.15)	6.32 (0.08)	6.35 (0.09)
K_2O	4.41	3.98 (0.11)	3.89 (0.09)	3.7 (0.05)	3.68 (0.50)	3.33 (0.04)	3.57 (0.03)
Li_2O^{**}	1.05	1.10	1.10	1.10	1.10	1.10	1.10
Ag_2O	-	-	0.53 (0.05)	2.0 (0.11)	1.64 (0.13)	6.00 (0.15)	-
P_2O_5	1.72	1.54 (0.17)	1.63 (0.12)	1.6 (0.14)	2.07 (0.21)	2.31 (0.09)	1.39 (0.06)
F	-	-	2.14 (0.11)	4.3 (0.09)	5.73 (0.09)	7.78 (0.11)	4.71 (0.10)
$B_2O_3^{**}$	1.83	1.81	2.0	2.0	2.00	2.00	2.00
$H_2O^{\approx}$	0	9.49	9.6	9.0 (0.5)	10.25 (0.52)	8.10 (0.2)	11.23 (0.43)
ASI (ASI^+)	1.06 (0.15)	1.05 (0.17)	1.05 (0.18)	1.05 (0.15)	1.10 (0.29)	1.08 (0.22)	1.32(0.88)
ASI_{Li} (ASI_{Li}^+)	0.86 (-0.50)	0.87(-0.54)	0.90 (-0.55)	0.90 (-0.58)	0.89 (-0.44)	0.87 (-0.51)	1.06 (0.15)
ASI_{eff}(ASI_{eff}^+)	0.94 (-0.27)	0.92 (-0.37)	0.91 (-0.42)	0.91 (-0.45)	0.96 (-0.27)	0.95 (-0.32)	1.0 (0.03)
Total	99.52	102	100.9	101.8	102.41	103.27	101.98

Microprobe analysis of the starting glasses. Oxides values in parentheses represent 2σ standard deviation. Li^{**} and B^{**} contents were determined in the dry starting glass by ICP/MS. In hydrous glasses, Li and B values were corrected. $H_2O^{\approx}$ content was estimated by taking the difference of the total oxides to 100 %. D.gls : anhydrous starting glass;0.gls: hydrous starting glass; 2-gls to 8-gls: starting glasses contain variable F concentration; gls^*: peraluminous glass where F was added as AlF_3. ASI is the molar ratio of Al/(Na+K); ASI^+ is the molar of Al-Na-K per kilogram; ASI_{Li} is the molar ratio of Al/(Na+K+Li); ASI_{Li}^+ is the molar of Al-Na-K-Li per kilogram; ASI_{eff} is the molar ratio of (Al±P)/(Na+K+Li); ASI_{eff}^+ is the molar of Al±P-Na-K-Li per kilogram (see the text for more information about P role).

Table 2-2 Mn-Columbite Solubility

experiments	T (C°)	P kbars	Duration (Days)	ASI	ASI^+	ASI_{Li}	ASI_{Li}^+	ASI_{eff}	ASI_{eff}^+	F wt.%	MnO wt.%	Nb2O5 wt. %	Mn/Nb	$logK_{Sp}^{MnNb}$ $_{mol^2/kg^2}$
SO.46	700	2	5	1.10	0.29	0.85	-0.76	0.89	-0.44	6	0.22 (0.01)	0.49 (0.02)	0.84 (0.05)	-3.24 (0.02)
Nb1	800	2	5	1.05	0.17	0.83	-0.67	0.88	-0.54	0	0.35 (0.02)	1.04 (0.03)	0.63 (0.05)	-2.72 (0.02)
Nb2	800	2	5	1.05	0.18	0.81	-0.73	0.87	-0.60	2	0.35 (0.03)	1.03 (0.06)	0.64 (0.06)	-2.72 (0.06)
Nb3	800	2	5	1.05	0.15	0.81	-0.74	0.86	-0.60	4	0.33 (0.03)	0.99 (0.03)	0.63 (0.06)	-2.75 (0.06)
Nb4	800	2	5	1.10	0.15	0.83	-0.60	0.91	-0.44	6	0.33 (0.04)	0.93 (0.15)	0.66 (0.08)	-2.79 (0.08)
SO.34	800	2	5	1.32	0.88	1.04	0.08	0.91	-0.04	6	0.15 (0.03)	0.39 (0.04)	0.73 (0.16)	-4.14 (0.04)
SO.42^R	800	2	5	1.06	0.15	0.83	-0.76	0.88	-0.53	0	0.33 (0.02)	0.86 (0.03)	0.72 (0.08)	-2.81 (0.02)
SO.38^R	800	2	5	1.07	0.15	0.83	-0.60	0.91	-0.53	6	0.31 (0.03)	0.75 (0.03)	0.77 (0.09)	-2.91 (0.03)
SO.1	1000	2	2	1.05	0.15	0.76	-0.98	0.81	-0.85	0	0.95 (0.03)	3.19 (0.04)	0.56 (0.02)	-1.79 (0.01)
SO.5	1000	2	2	1.10	0.15	0.84	-0.97	0.83	-0.84	6	0.97 (0.01)	3.28 (0.04)	0.55 (0.01)	-1.77 (0.01)

Microprobe analysis of Mn-columbite solubility. Values in parentheses represent 2σ standard deviation. R: reverse experiments. ASI is the molar ratio of Al/(Na+K); ASI^+ is the molar of Al-Na-K- per kilogram; ASI_{Li} is the molar ratio of Al/(Na+K+Li+2Mn); ASI_{Li}^+ is the molar of Al-Na-K-Li-2Mn per kilogram; ASI_{eff} is the molar ratio of (Al±P)/(Na+K+Li+2Mn); ASI_{eff}^+ is the molar of Al±P-Na-K-Li-2Mn per kilogram (see the text for more information about P role).

Table 2-3 Mn-Tantalite Solubility

experiments	T (C°)	P kbars	Duration (Days)	ASI	ASI^+	ASI_{Li}	ASI_{Li}^+	ASI_{eff}	ASI_{eff}^+	F wt.%	MnO wt.%	Ta2O5 wt. %	Mn/Ta	$logK_{Sp}^{MnTa}$ $_{mol^2/kg^2}$
SO.47	700	2	5	1.10	0.29	0.84	-0.55	0.89	-0.38	6	0.22 (0.02)	2.46 (0.15)	0.28 (0.20)	-2.75 (0.02)
Ta1	800	2	5	1.05	0.17	0.81	-0.76	0.96	-0.63	0	0.52 (0.05)	2.77 (0.11)	0.58 (0.06)	-2.34 (0.06)
Ta2	800	2	5	1.05	0.15	0.79	-0.81	0.89	-0.68	2	0.52 (0.02)	2.73 (0.06)	0.59 (0.03)	-2.34 (0.03)
Ta3	800	2	5	1.05	0.15	0.78	-0.84	0.84	-0.71	4	0.52 (0.03)	2.55 (0.09)	0.64 (0.04)	-2.37 (0.04)
Ta4	800	2	5	1.10	0.15	0.81	-0.51	0.88	-0.32	6	0.53 (0.03)	2.33 (0.11)	0.70 (0.05)	-2.41 (0.04)
SO.35	800	2	5	1.32	0.88	1.00	0.04	0.95	-0.07	6	0.22 (0.01)	1.37 (0.04)	0.50 (0.05)	-2.99 (0.04)
SO.43^R	800	2	5	1.04	0.15	0.81	-0.72	0.86	-0.60	0	0.46 (0.01)	2.42 (0.05)	0.60 (0.01)	-2.45 (0.01)
SO.39^R	800	2	5	1.10	0.15	0.82	-0.67	0.89	-0.50	6	0.46 (0.01)	2.43 (0.05)	0.60 (0.01)	-2.44 (0.01)
SO.2	1000	2	2	1.05	0.15	0.76	-0.98	0.81	-0.85	0	0.97 (0.02)	6.13 (0.05)	0.49 (0.01)	-1.72 (0.01)
SO.6	1000	2	2	1.10	0.15	0.76	-0.90	0.83	-0.74	6	0.93 (0.02)	5.87 (0.12)	0.49 (0.01)	-1.76 (0.01)

Microprobe analysis of Mn-tantalite solubility. Values in parentheses represent 2σ standard deviation. R: reverse experiments. ASI is the molar ratio of Al/(Na+K); ASI^+ is the molar of Al-Na-K- per kilogram; ASI_{Li} is the molar ratio of Al/(Na+K+Li+2Mn); ASI_{Li}^+ is the molar of Al-Na-K-Li-2Mn per kilogram; ASI_{eff} is the molar ratio of (Al±P)/(Na+K+Li+2Mn); ASI_{eff}^+ is the molar of Al±P-Na-K-Li-2Mn per kilogram (see the text for more information about P role).

Table 2-4 Zircon solubility

experiments	T (C°)	P kbars	Duration (Days)	ASI	ASI_{Li}	ASI_{eff}	ASI_{eff}^{+}	F wt.%	ZrO_2 wt.%	ZrO_2 mol/kg 10^{-3}
Zr1	800	2	5	1.05	0.87	0.92	-0.37	0	0.25(0.04)	0.20 (0.4)
Zr2	800	2	5	1.10	0.90	0.91	-0.42	2	0.26 (0.02)	0.24 (0.2)
Zr3	800	2	5	1.10	0.90	0.91	-0.45	4	0.37 (0.03)	0.30 (0.3)
Zr4	800	2	5	1.10	0.89	0.96	-0.27	6	0.38 (0.03)	0.31 (0.3)
SO.26	800	2	5	1.08	0.87	0.95	-0.32	8	0.47 (0.03)	0.38 (0.3)
$SO.44^{R}$	800	2	5	1.05	0.87	0.92	-0.37	0	0.24 (0.01)	0.20 (0.1)
$SO.40^{R}$	800	2	5	1.04	0.89	0.96	-0.27	6	0.40 (0.02)	0.33 (0.2)
SO.3	1000	2	2	1.05	0.87	0.92	-0.37	0	0.65 (0.02)	0.53 (0.2)
SO.4	1000	2	2	1.08	0.90	0.96	-0.27	6	0.94 (0.02)	0.28 (0.2)

Microprobe analysis of zircon solubility. Values in parentheses represent 2σ standard deviation. R: reverse experiments. ASI is the molar ratio of Al/(Na+K); ASI_{Li} is the molar ratio of Al/(Na+K+Li); ASI_{eff} is the molar ratio of (Al±P)/(Na+K+Li); ASI_{eff}^{+} is the molar of Al±P-Na-K-Li per kilogram (see the text for more information about P role).

Table 2-5 Hafnon Solubility

experiments	T (C°)	P kbars	Duration (Days)	ASI	ASI_{Li}	ASI_{eff}	ASI_{eff}^{+}	F wt.%	HfO_2 wt.%	HfO_2 mol/kg 10^{-3}
Hf1	800	2	5	1.05	0.87	0.92	-0.37	0	0.85(0.05)	0.40 (0.3)
Hf2	800	2	5	1.10	0.90	0.91	-0.42	2	0.95 (0.11)	0.45 (0.7)
Hf3	800	2	5	1.10	0.90	0.91	-0.45	4	1.08 (0.18)	0.51 (1.2)
Hf4	800	2	5	1.10	0.89	0.96	-0.27	6	1.16 (0.11)	0.55 (0.7)
SO.37	800	2	5	1.32	1.06	1.0	0.03	4.7	0.37 (0.06)	0.18 (0.4)
SO.27	800	2	5	1.05	0.87	0.92	-0.37	8	1.30 (0.09)	0.62 (0.6)
$SO.45^{R}$	800	2	5	1.04	0.89	0.96	-0.27	0	0.85 (0.05)	0.40 (0.3)
SO.7	1000	2	2	1.05	0.87	0.92	-0.37	0	1.62 (0.10)	0.77(0.6)
SO.8	1000	2	2	1.08	0.90	0.96	-0.27	6	1.92 (0.08)	0.63 (0.5)

Microprobe analysis of hafnon solubility. Values in parentheses represent 2σ standard deviation. R: reverse experiments. ASI is the molar ratio of Al/(Na+K); ASI_{Li} is the molar ratio of Al/(Na+K+Li); ASI_{eff} is the molar ratio of (Al±P)/(Na+K+Li); ASI_{eff}^{+} is the molar of Al±P-Na-K-Li per kilogram (see the text for more information about P role).

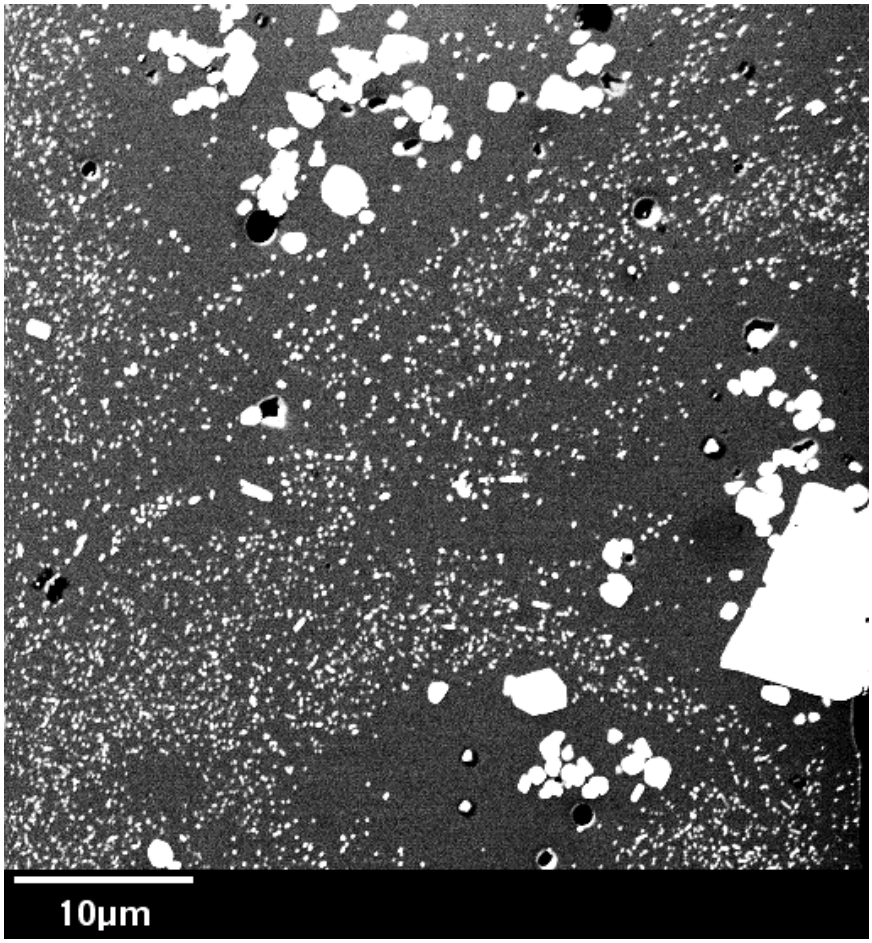

Figure 2-1 Backscattered image of Mn-columbite reversal experiment (SO.43R) at 800 °C and 2 kbars. Very fine crystals formed during crystallization experiments. The clean areas around the large seed crystals were used to acquiring EMP analysis

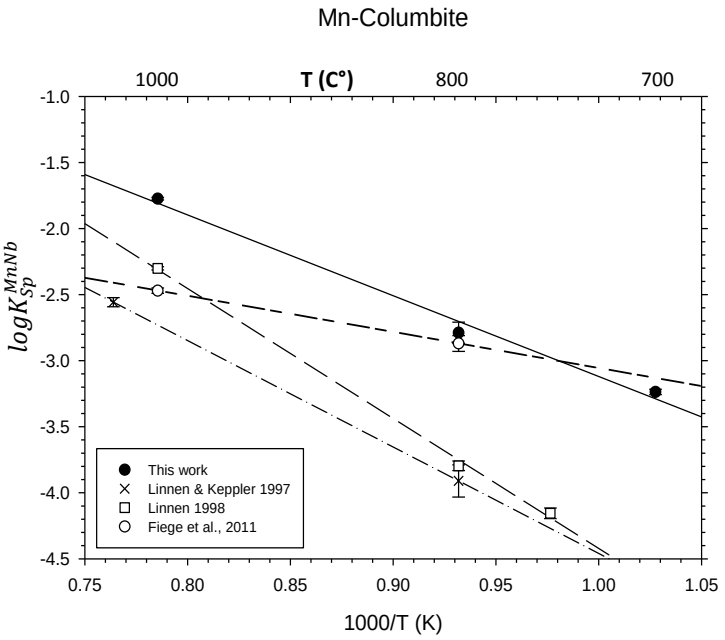

Figure 2-3 Temperature dependence of Mn-columbite in water saturated haplogranitic melts at 2 kbars. The solid squares represent the data obtained from dissolution experiments and the solid circles represent the data of the 1000 and 800 °C dissolution experiments and the extrapolated value of experiment at 700 °C. The open triangles represent data of Linnen and Keppler (1997) and the open squares represent the data of Fiege et al (2011), which were plotted here for comparison.

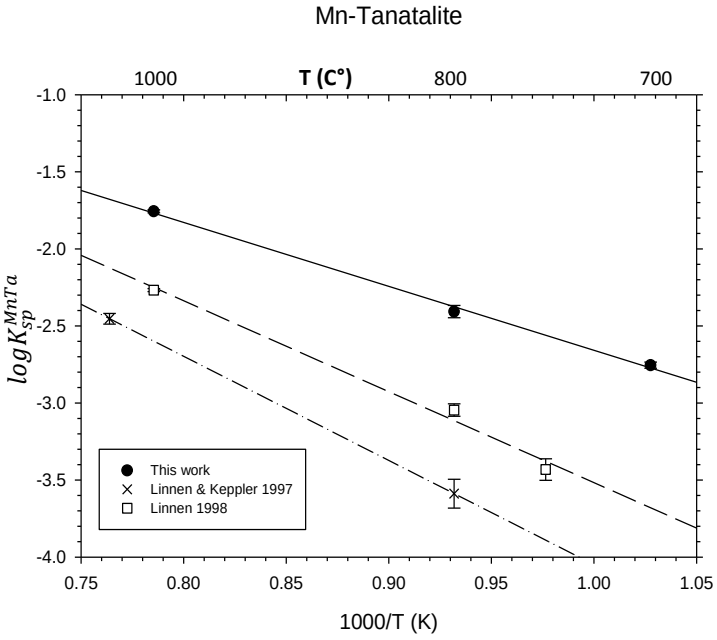

Figure 2-3 Temperature dependence of Mn-tantalite in water saturated haplogranitic melts at 2 kbars. The solid squares represent the data obtained from dissolution experiments and the solid circles represent the data of the 1000 and 800 °C dissolution experiments and the extrapolated value of experiment at 700 °C. The open triangles represent data of Linnen and Keppler (1997), which was plotted here for comparison.

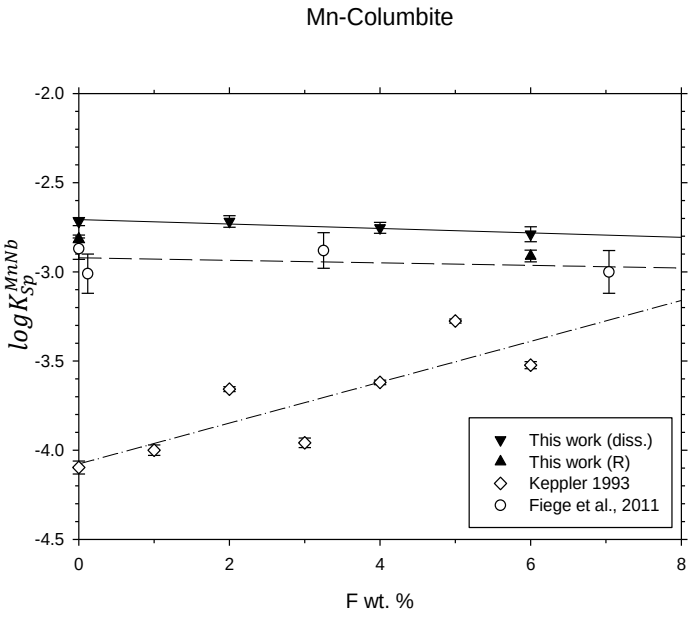

Figure 2-4 Fluorine effect on the solubility of Mn-columbite. This work results (solid symbols) show that fluorine has no effect on the solubility products of Mn-columbite (solid inverted triangles for dissolution experiments and upward solid triangles are for crystallization experiments The abbreviations diss. and R stand for dissolution and reverse experiments, respectively.) which supports the previous study of Fiege et al. (2011) (open circles). The open diamonds represent the study of Keppler (1993).

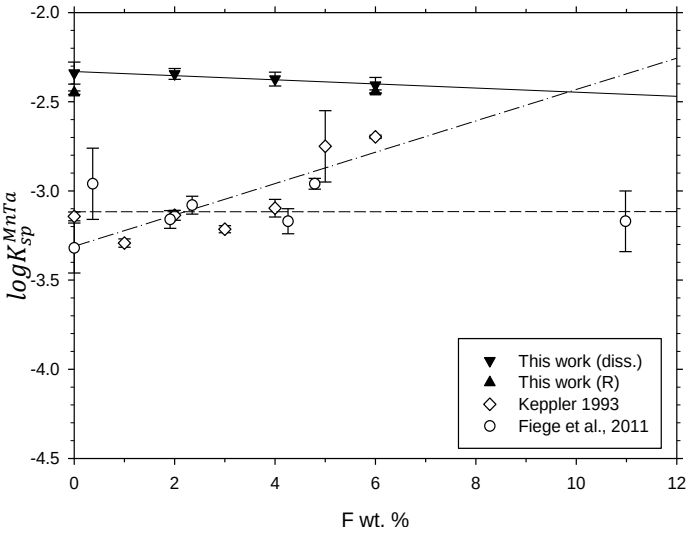

Figure 2-4 Fluorine effect on the solubility of Mn-tantalite. This work results (solid symbols) show that fluorine has no effect on the solubility products of Mn-tantalite (solid inverted triangles are for dissolution experiments and upward solid triangles are for crystallization experiments. The abbreviations diss. and R stand for dissolution and reverse experiments, respectively.), which supports the previous study of Fiege et al. (open circles, 2011). The open diamonds represent the study of Keppler (1993).

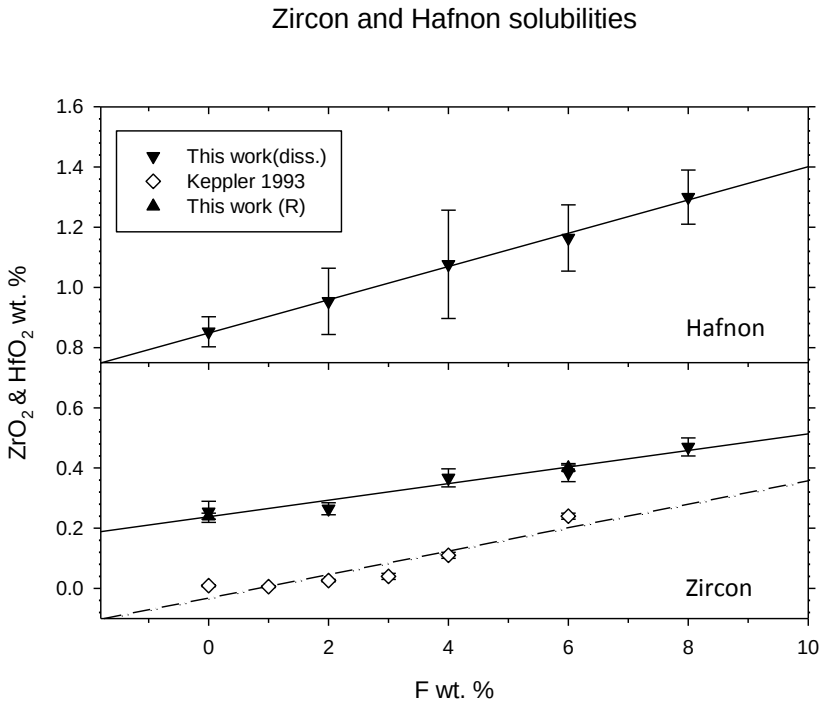

Figure 2-5 Fluorine effect on the solubilities of zircon and hafnon. This work results (solid inverted triangles for Zr dissolution experiments, upward triangles for Zr crystallization experiments) show that solubility increases with increasing the fluorine concentration in the melt, and that supports Keppler (open diamonds ,1993).

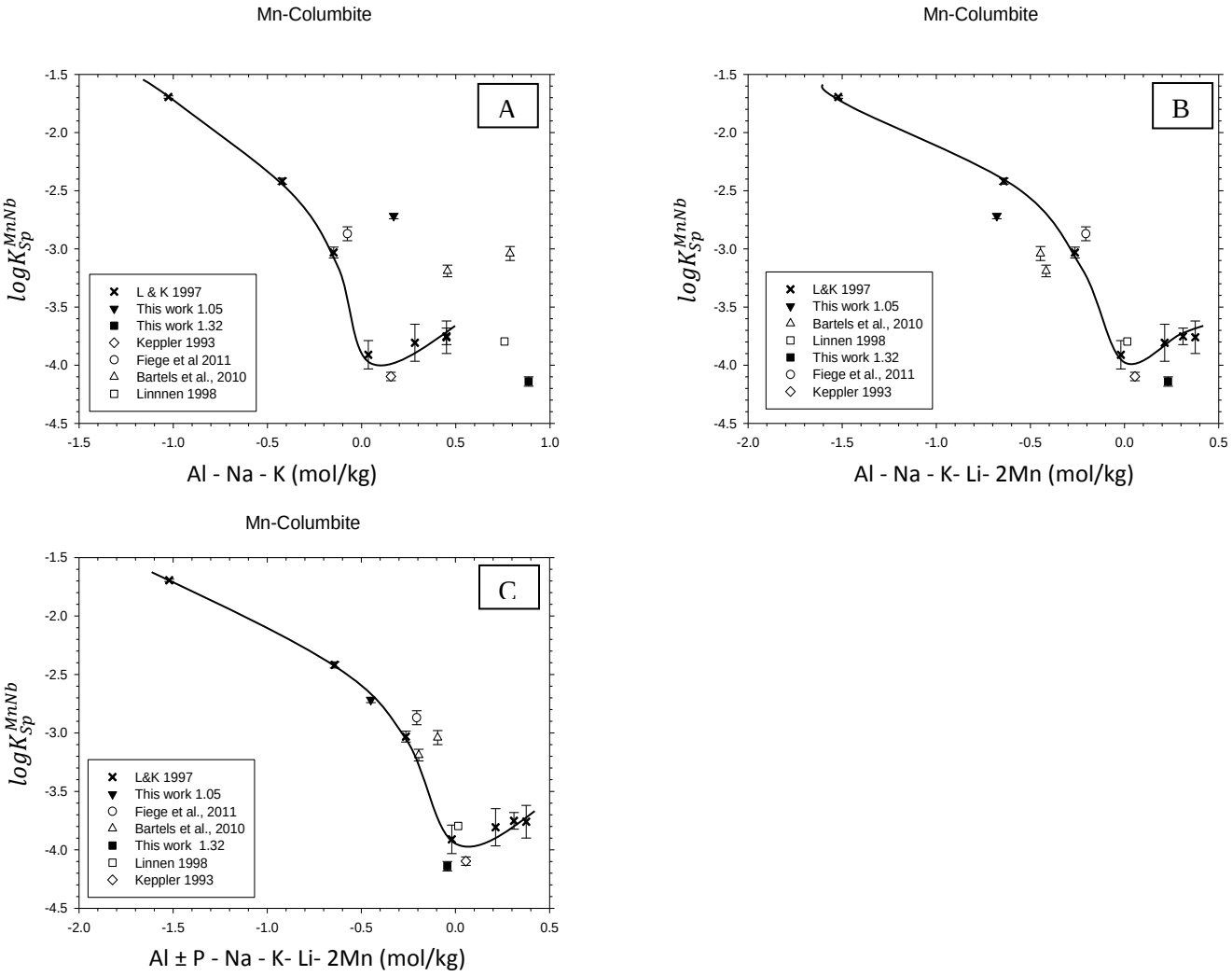

Figure 2-6 The effect of melt composition on the solubility of Mn-columbite at 800 C° and 2 kbars. The data of Linnen and Keppler (X symbols, 1997) were plotted here for comparison. Other data point for similar melt plotted as well. The values (1.05 and 1.32) of this work represent the ASI values of the glasses. The curve is from Linnen and Keppler (1997). The solubility products plotted against ASI^{+} in **A**, ASI_{Li}^{+} in **B** and ASI_{eff}^{+} in **C**. (see the text for more discussion).

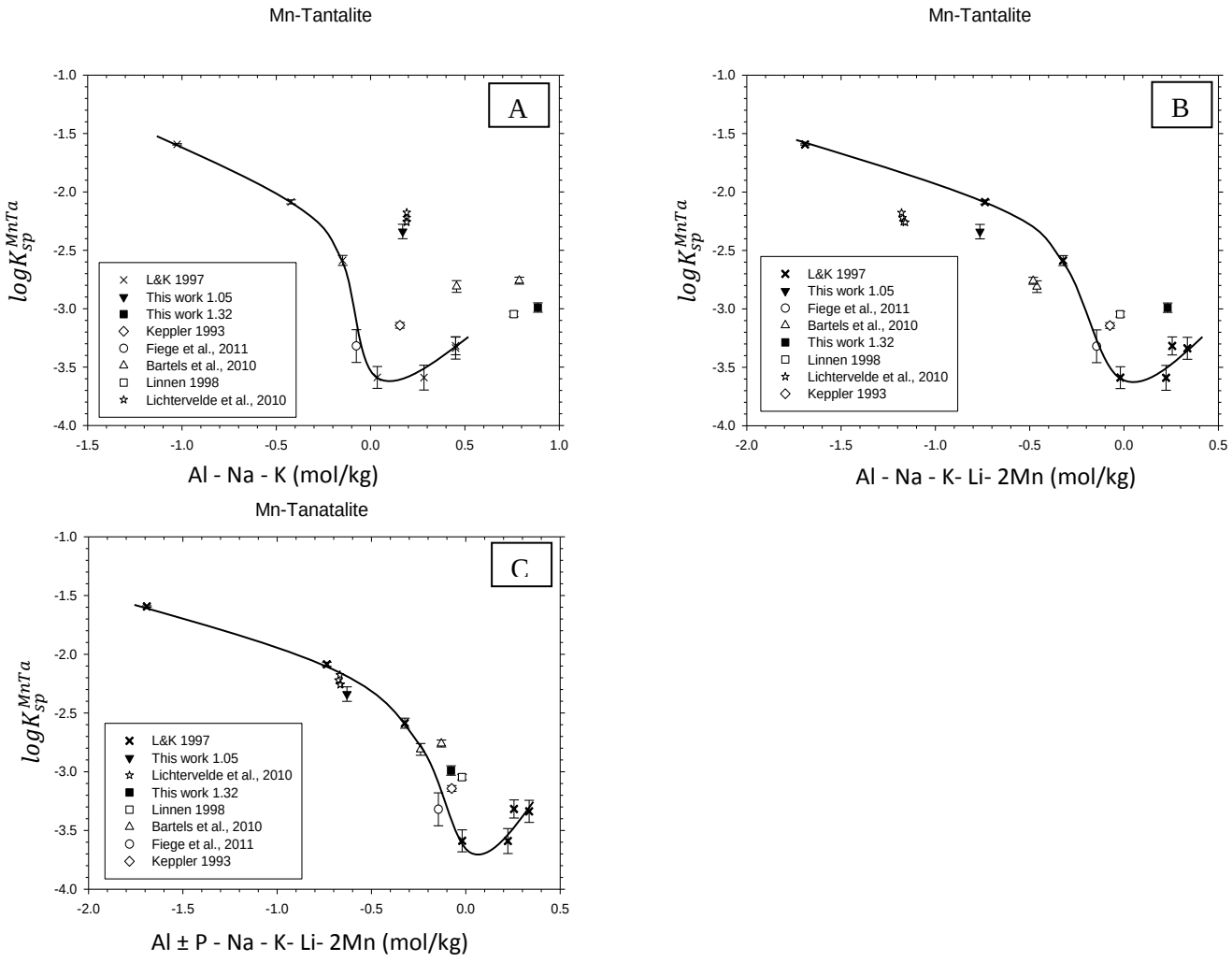

Figure 2-7 The effect of melt composition on the solubility of Mn-tantalite at 800 C° and 2 kbars. The data of Linnen and Keppler (X symbols, 1997) were plotted here for comparison. Other data point for similar melt plotted as well. The values (1.05 and 1.32) of this work represent the ASI values of the glasses. The curve is from Linnen and Keppler (1997). The solubility products plotted against ASI^{+} in **A**, ASI_{Li}^{+} in **B** and ASI_{eff}^{+} in **C** (see the text for more

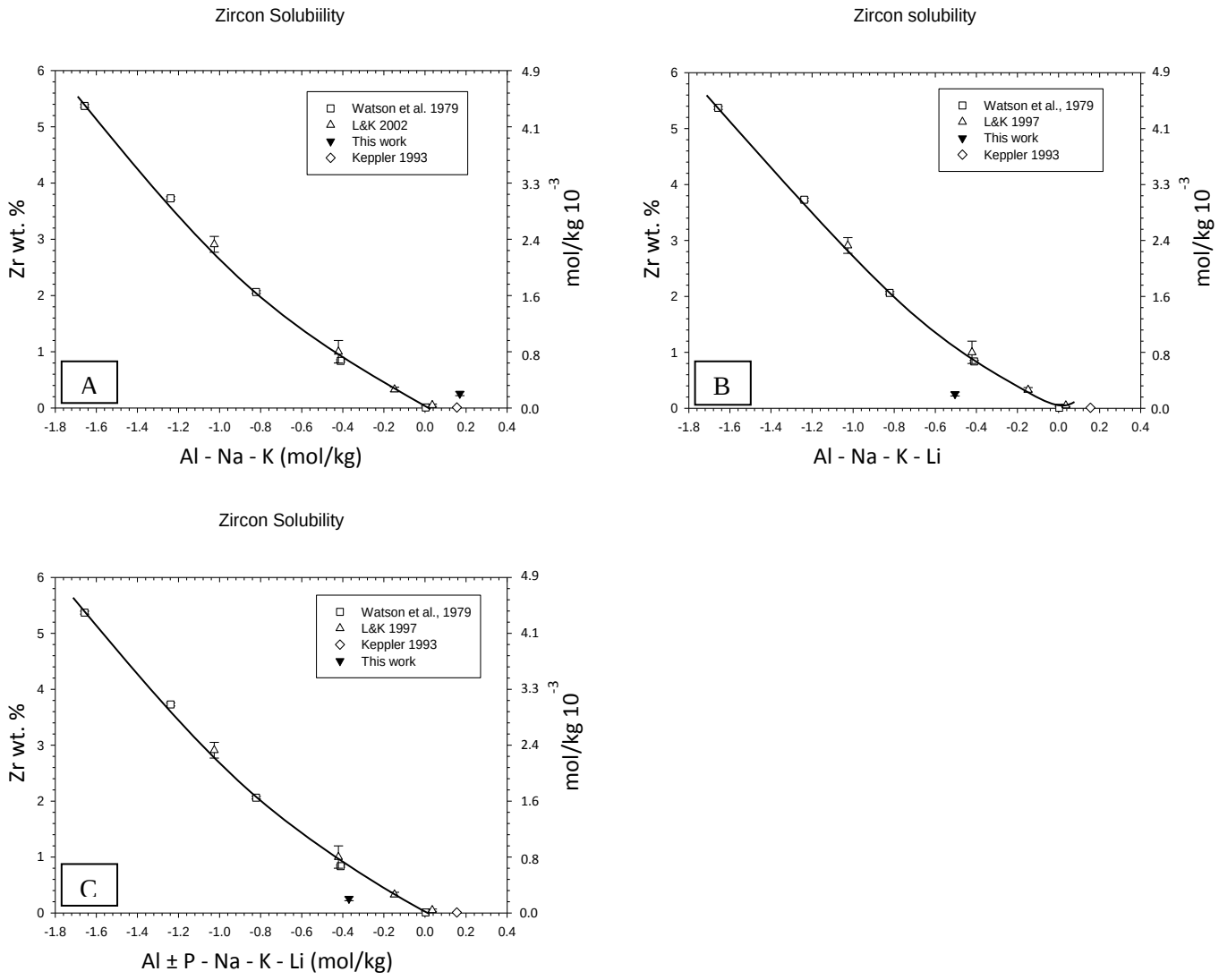

Figure 2-8 Comparison of zircon solubility of this work (solid inverted triangle ASI=1.05) to previous studies. the curve is from Watson (1979) study. The solubility products plotted against ASI^{+} in **A**, ASI_{Li}^{+} in **B** and ASI_{eff}^{+} in **C**.

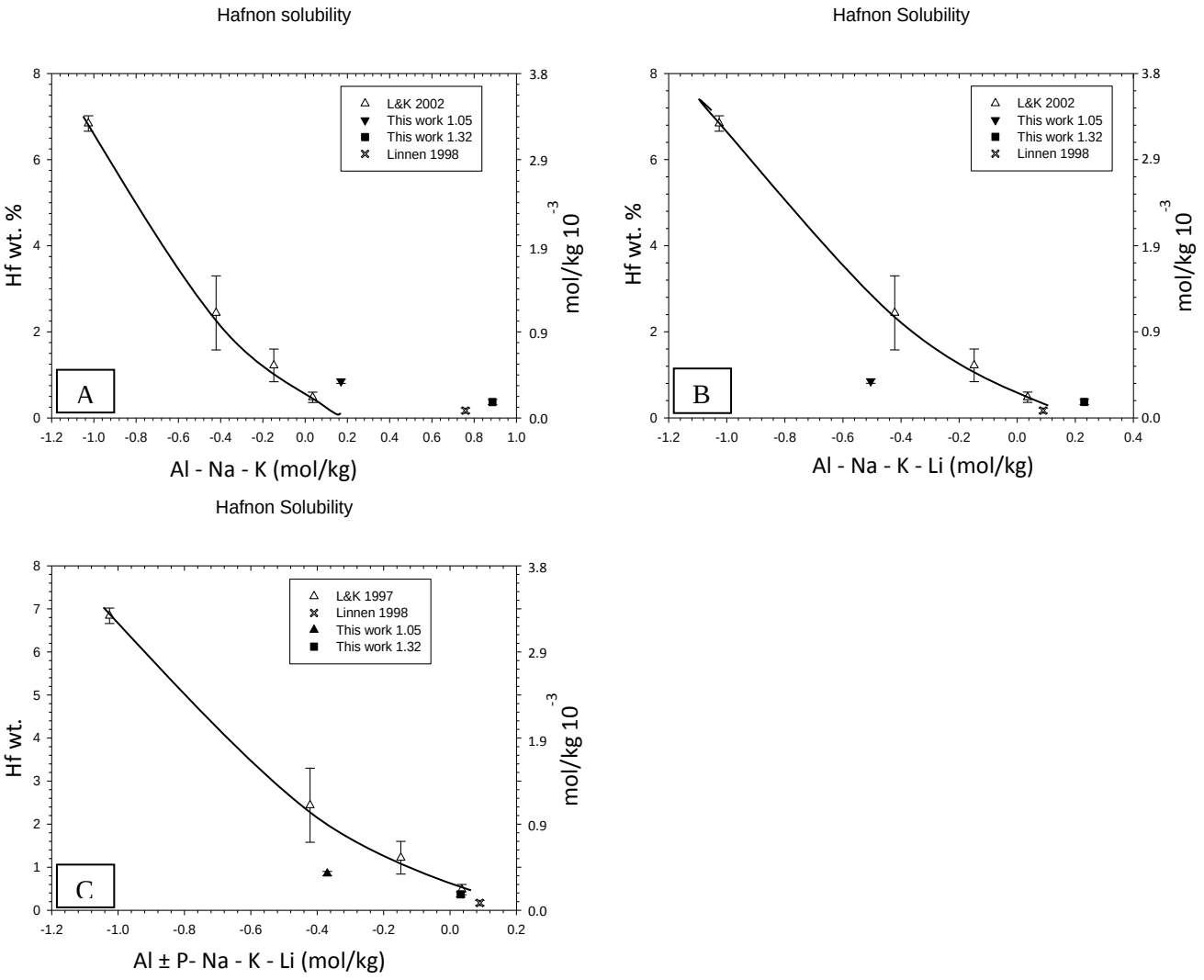

Figure 2-9 Comparison of hafnon solubility of this work (solid inverted triangle ASI=1.05 and solid square ASI=1.32) to previous studies. the curve is from Linnen and Keppler (2002) study. The solubility products plotted against ASI^{+} in **A**, $ASI_{Li}{}^{+}$ in **B** and $ASI_{eff}{}^{+}$ in **C**.

Appendix A

Starting glasses analysis

Starting glasses, high temperature and reverse experiments analysis was done at CANMET laboratory, Ottawa, Ontario, Canada. Li and B values are fixed (Fix) and assumed to be the same as their values measured by ICP/MS. The concentration of H_2O was taken by the difference.

- Acc. V : 15 kV; current: 15 nA, beam defocused at 35-40 microns; counting times 10 to 20 seconds on peak and background.
- alkali and F X-ray intensities as a function of time were monitored to ensure that there is no mobility with the analytical conditions used.
- uncertainty represents 3 times the standard deviation based on counting statistics.

											Fix	*Fix*	*by diff.*	
D-glass	SiO_2	+/-	Al_2O_3	+/-	Na_2O	+/-	K_2O	+/-	P_2O_5	+/-	*Li_2O*	*B_2O_3*	*H_2O*	Total
Location 1	63.42	1.00	17.56	0.29	8.15	0.34	4.47	0.12	1.63	0.18	1.1	2	1.7	100.00
Location 2	62.90	0.99	17.68	0.29	8.46	0.35	4.47	0.12	1.78	0.18	1.1	2	1.6	100.00
Location 3	62.68	0.99	18.21	0.30	8.28	0.35	4.51	0.12	1.82	0.19	1.1	2	1.4	100.00
Location 4	63.64	1.00	17.88	0.29	8.49	0.35	4.55	0.12	1.75	0.18	1.1	2	0.6	100.00
Location 5	65.96	1.02	16.84	0.28	7.66	0.34	4.55	0.12	1.25	0.16	1.1	2	0.6	100.00
Location 6	62.30	0.99	18.97	0.30	8.59	0.36	4.58	0.12	1.88	0.19	1.1	2	0.6	100.00
Location 7	64.12	1.00	17.25	0.29	8.11	0.35	4.51	0.12	1.98	0.19	1.1	2	0.9	100.00
Location 8	63.54	1.00	18.39	0.30	8.10	0.34	4.62	0.12	1.78	0.18	1.1	2	0.5	100.00
Location 9	63.80	1.00	17.84	0.29	7.96	0.34	4.54	0.12	1.65	0.18	1.1	2	1.1	100.00
Location 10	63.41	1.00	17.90	0.29	8.27	0.35	4.51	0.12	1.67	0.18	1.1	2	1.1	100.00
Location 11	63.20	1.00	17.99	0.29	8.24	0.35	4.54	0.12	1.81	0.19	1.1	2	1.1	100.00
Location 12	63.12	1.00	17.66	0.29	7.90	0.34	4.57	0.12	1.55	0.17	1.1	2	2.1	100.00
Location 13	62.12	0.99	18.70	0.30	8.60	0.36	4.53	0.12	1.85	0.19	1.1	2	1.1	100.00
Location 14	63.84	1.00	17.44	0.29	7.98	0.34	4.50	0.12	1.64	0.18	1.1	2	1.5	100.00
Location 15	62.27	0.99	18.36	0.30	8.44	0.35	4.52	0.12	2.25	0.21	1.1	2	1.1	100.00
Ave.	63.4	1.0	17.9	0.3	8.2	0.3	4.5	0.1	1.8	0.2	1.1	2.0	1.1	100.0
std	0.9	0.0	0.6	0.0	0.3	0.0	0.0	0.0	0.2	0.0	0.0	0.0	0.5	0.0

H-glass	SiO_2	+/-	Al_2O_3	+/-	Na_2O	+/-	K_2O	+/-	P_2O_5	+/-	Li_2O	B_2O_3	H_2O	Total
Location 1	57.28	0.95	16.98	0.29	7.19	0.33	3.97	0.11	1.50	0.17	1.1	2	10.0	100.00
Location 2	57.16	0.95	16.93	0.29	7.22	0.33	3.96	0.11	1.55	0.17	1.1	2	10.1	100.00
Location 3	58.04	0.96	16.91	0.29	7.29	0.33	3.95	0.11	1.69	0.18	1.1	2	9.0	100.00
Location 4	57.78	0.95	17.08	0.29	7.30	0.33	4.02	0.11	1.53	0.17	1.1	2	9.2	100.00
Location 5	57.61	0.95	17.00	0.29	7.34	0.33	3.97	0.11	1.60	0.17	1.1	2	9.4	100.00
Location 6	57.50	0.95	16.94	0.29	7.11	0.33	4.00	0.11	1.43	0.16	1.1	2	9.9	100.00
Location 7	57.29	0.95	16.85	0.28	7.32	0.33	4.00	0.11	1.51	0.17	1.1	2	9.9	100.00
Location 8	57.60	0.95	16.84	0.28	7.12	0.33	3.94	0.11	1.57	0.17	1.1	2	9.8	100.00
Location 9	57.79	0.95	17.37	0.29	7.13	0.33	3.96	0.11	1.47	0.17	1.1	2	9.2	100.00
Location 10	57.00	0.95	18.51	0.30	7.53	0.34	4.01	0.11	1.49	0.17	1.1	2	8.4	100.00
Ave.	59.3	1.0	17.4	0.3	7.6	0.3	4.2	0.1	1.6	0.2	1.1	2.0	6.8	100.0
std	2.7	0.0	0.7	0.0	0.5	0.0	0.3	0.0	0.2	0.0	0.0	0.0	4.0	0.0

- Acc. V : 15 kV; current: 15 nA, beam defocused at 35-40 microns; counting times 10 to 20 seconds on peak and background.
- alkali and F X-ray intensities as a function of time were monitored to ensure that there is no mobility with the analytical conditions used.
- uncertainty represents 3 times the standard deviation based on counting statistics.

																Fix	*Fix*	*by diff.*	
8wt % F glass	SiO_2	+/-	Al_2O_3	+/-	Na_2O	+/-	K_2O	+/-	Ag_2O	+/-	P_2O_5	+/-	F	+/-	*Li_2O*	*B_2O_3*	*H_2O*	Total
1	51.46	0.91	15.02	0.27	6.19	0.32	3.35	0.10	5.86	0.29	2.13	0.20	7.50	0.25	*1.1*	*2.0*	*8.6*	100.00
2	50.99	0.90	15.26	0.28	6.28	0.32	3.35	0.10	6.10	0.30	2.39	0.21	7.89	0.26	*1.1*	*2.0*	*8.0*	100.00
3	51.32	0.90	15.22	0.28	6.44	0.33	3.32	0.10	6.05	0.34	2.33	0.21	7.69	0.26	*1.1*	*2.0*	*7.8*	100.00
4	51.06	0.90	15.17	0.28	6.38	0.33	3.37	0.10	6.03	0.34	2.29	0.20	7.69	0.26	*1.1*	*2.0*	*8.1*	100.00
5	51.14	0.90	15.33	0.28	6.42	0.33	3.27	0.10	5.96	0.34	2.24	0.20	7.91	0.26	*1.1*	*2.0*	*8.0*	100.00
6	51.22	0.90	15.16	0.27	6.35	0.32	3.33	0.10	6.00	0.34	2.17	0.20	7.87	0.26	*1.1*	*2.0*	*8.1*	100.00
7	51.74	0.91	15.02	0.27	6.25	0.32	3.28	0.10	5.66	0.33	2.27	0.20	7.78	0.26	*1.1*	*2.0*	*8.2*	100.00
8	50.99	0.90	15.32	0.28	6.32	0.32	3.35	0.10	5.88	0.33	2.37	0.21	7.90	0.26	*1.1*	*2.0*	*8.1*	100.00
9	51.36	0.90	15.17	0.27	6.24	0.32	3.36	0.10	5.82	0.33	2.20	0.20	7.71	0.26	*1.1*	*2.0*	*8.3*	100.00
10	51.13	0.90	15.13	0.28	6.27	0.32	3.28	0.10	6.17	0.34	2.37	0.21	7.77	0.26	*1.1*	*2.0*	*8.0*	100.00
11	50.73	0.90	15.15	0.28	6.36	0.33	3.36	0.10	6.12	0.34	2.35	0.21	7.71	0.26	*1.1*	*2.0*	*8.4*	100.00
12	50.80	0.90	15.23	0.28	6.38	0.33	3.37	0.10	6.26	0.35	2.35	0.21	7.76	0.26	*1.1*	*2.0*	*8.0*	100.00
13	51.49	0.90	14.92	0.27	6.20	0.32	3.36	0.10	6.04	0.34	2.39	0.21	7.80	0.26	*1.1*	*2.0*	*8.0*	100.00
14	51.33	0.90	15.05	0.27	6.35	0.32	3.38	0.10	6.06	0.34	2.36	0.21	7.83	0.26	*1.1*	*2.0*	*7.8*	100.00
15	51.20	0.90	15.01	0.27	6.39	0.32	3.28	0.10	5.95	0.34	2.40	0.21	7.82	0.26	*1.1*	*2.0*	*8.1*	100.00
Ave.	51.2	0.9	15.1	0.3	6.3	0.3	3.3	0.1	6.0	0.3	2.3	0.2	7.8	0.3	1.1	2.0	8.1	100.0
std	0.3	0.0	0.1	0.0	0.1	0.0	0.0	0.0	0.2	0.0	0.1	0.0	0.1	0.0	0.0	0.0	0.2	0.0
6wt % F glass	SiO_2	+/-	Al_2O_3	+/-	Na_2O	+/-	K_2O	+/-	Ag_2O	+/-	P_2O_5	+/-	F	+/-	*Li_2O*	*B_2O_3*	*H_2O*	Total
1	54.43	0.93	16.12	0.28	6.70	0.33	3.70	0.11	1.71	0.16	1.83	0.19	5.79	0.23	*1.1*	*2.0*	*9.1*	100.00
2	53.90	0.92	16.14	0.28	6.18	0.31	3.78	0.11	1.78	0.17	1.98	0.19	5.74	0.23	*1.1*	*2.0*	*9.8*	100.00

3	54.09	0.92	16.01	0.28	6.56	0.32	3.64	0.11	1.70	0.17	2.16	0.20	5.74	0.23	*1.1*	*2.0*	*9.4*	100.00
4	53.20	0.91	15.71	0.28	6.42	0.32	3.59	0.11	1.59	0.16	2.52	0.21	5.81	0.23	*1.1*	*2.0*	*10.5*	100.00
5	53.25	0.92	15.79	0.28	6.36	0.32	3.67	0.11	1.74	0.17	2.37	0.21	5.82	0.23	*1.1*	*2.0*	*10.3*	100.00
6	53.76	0.92	15.88	0.28	6.44	0.32	3.64	0.11	1.30	0.15	2.12	0.20	5.67	0.23	*1.1*	*2.0*	*10.5*	100.00
7	53.74	0.92	16.03	0.28	6.42	0.32	3.75	0.11	1.62	0.16	2.05	0.19	5.80	0.23	*1.1*	*2.0*	*9.9*	100.00
8	53.56	0.92	15.99	0.28	6.22	0.32	3.68	0.11	1.56	0.16	1.85	0.19	5.72	0.23	*1.1*	*2.0*	*10.7*	100.00
9	53.47	0.92	15.99	0.28	6.23	0.32	3.67	0.11	1.80	0.17	1.92	0.19	5.58	0.23	*1.1*	*2.0*	*10.6*	100.00
10	53.30	0.92	16.04	0.28	6.25	0.32	3.61	0.11	1.59	0.16	1.91	0.19	5.58	0.23	*1.1*	*2.0*	*11.0*	100.00
11	53.49	0.92	15.77	0.28	6.34	0.32	3.68	0.11	1.68	0.16	2.35	0.21	5.88	0.23	*1.1*	*2.0*	*10.2*	100.00
12	53.02	0.92	15.95	0.28	6.23	0.32	3.64	0.11	1.72	0.17	2.16	0.20	5.75	0.23	*1.1*	*2.0*	*10.8*	100.00
13	53.69	0.92	15.92	0.28	6.56	0.32	3.73	0.11	1.68	0.16	1.89	0.19	5.65	0.23	*1.1*	*2.0*	*10.2*	100.00
14	53.50	0.92	16.13	0.28	6.29	0.32	3.70	0.11	1.48	0.15	1.97	0.19	5.77	0.23	*1.1*	*2.0*	*10.5*	100.00
15	53.80	0.92	15.96	0.28	6.43	0.32	3.68	0.11	1.65	0.16	1.96	0.19	5.72	0.23	*1.1*	*2.0*	*10.1*	100.00
Ave.	53.6	0.9	16.0	0.3	6.4	0.3	3.7	0.1	1.6	0.2	2.1	0.2	5.7	0.2	1.1	2.0	10.2	100.0
std	0.4	0.0	0.1	0.0	0.1	0.0	0.1	0.0	0.1	0.0	0.2	0.0	0.1	0.0	0.0	0.0	0.5	0.0

6wt % F AlF₃	SiO_2	+/-	Al_2O_3	+/-	Na_2O	+/-	K_2O	+/-	Ag_2O	+/-	P_2O_5	+/-	F	+/-	*Li_2O*	*B_2O_3*	*H_2O*	Total
1	53.01	0.91	18.52	0.30	6.25	0.31	3.56	0.10	-0.02	-0.07	1.33	0.16	4.56	0.21	*1.1*	*2.0*	*11.6*	100.00
2	52.98	0.92	18.65	0.30	6.33	0.31	3.55	0.11	0.01	0.06	1.40	0.16	4.55	0.21	*1.1*	*2.0*	*11.3*	100.00
3	53.28	0.92	18.74	0.30	6.24	0.31	3.52	0.10	-0.01	-0.02	1.43	0.16	4.72	0.21	*1.1*	*2.0*	*11.0*	100.00
4	53.46	0.92	18.81	0.30	6.41	0.32	3.59	0.11	-0.01	-0.03	1.35	0.16	4.60	0.21	*1.1*	*2.0*	*10.6*	100.00
5	52.94	0.92	18.83	0.30	6.19	0.31	3.60	0.11	0.02	0.07	1.37	0.16	4.76	0.21	*1.1*	*2.0*	*11.2*	100.00
6	52.20	0.91	19.04	0.30	6.26	0.31	3.60	0.11	0.01	0.07	1.27	0.16	4.67	0.21	*1.1*	*2.0*	*11.8*	100.00
7	52.31	0.91	18.86	0.30	6.45	0.32	3.57	0.11	0.00	0.00	1.41	0.16	4.86	0.21	*1.1*	*2.0*	*11.5*	100.00
8	52.33	0.91	18.98	0.30	6.37	0.31	3.61	0.11	-0.03	-0.08	1.38	0.16	4.70	0.21	*1.1*	*2.0*	*11.5*	100.00
9	52.52	0.91	18.70	0.30	6.38	0.31	3.57	0.11	0.03	0.06	1.44	0.16	4.70	0.21	*1.1*	*2.0*	*11.5*	100.00
10	53.02	0.92	18.71	0.30	6.32	0.31	3.52	0.10	-0.03	-0.08	1.31	0.16	4.69	0.21	*1.1*	*2.0*	*11.3*	100.00
11	53.15	0.92	18.94	0.30	6.33	0.31	3.57	0.11	0.02	0.07	1.51	0.17	4.68	0.21	*1.1*	*2.0*	*10.7*	100.00
12	53.48	0.93	18.87	0.30	6.50	0.32	3.58	0.11	-0.01	-0.03	1.42	0.16	4.66	0.21	*1.1*	*2.0*	*10.3*	100.00
13	52.50	0.91	18.75	0.30	6.28	0.31	3.57	0.11	-0.06	-0.19	1.49	0.17	4.88	0.21	*1.1*	*2.0*	*11.5*	100.00
14	52.17	0.91	19.09	0.30	6.42	0.31	3.56	0.11	-0.01	-0.02	1.41	0.16	4.80	0.21	*1.1*	*2.0*	*11.5*	100.00
15	52.92	0.92	18.89	0.30	6.44	0.32	3.62	0.11	0.02	0.07	1.34	0.16	4.72	0.21	*1.1*	*2.0*	*10.9*	100.00
Ave.	52.8	0.9	18.8	0.3	6.3	0.3	3.6	0.1	0.0	0.0	1.4	0.2	4.7	0.2	1.1	2.0	11.2	100.0
std	0.4	0.0	0.2	0.0	0.1	0.0	0.0	0.0	0.0	0.1	0.1	0.0	0.1	0.0	0.0	0.0	0.4	0.0
4wt % F glass	SiO_2	+/-	Al_2O_3	+/-	Na_2O	+/-	K_2O	+/-	Ag_2O	+/-	P_2O_5	+/-	F	+/-	*Li_2O*	*B_2O_3*	*H_2O*	Total
1	53.95	0.93	16.41	0.28	6.90	0.33	3.76	0.11	2.09	0.18	1.56	0.17	4.37	0.18	1.1	2.0	9.7	100.00
2	54.35	0.93	16.32	0.28	6.87	0.33	3.74	0.11	2.03	0.18	1.58	0.17	4.40	0.18	1.1	2.0	9.5	100.00
3	54.02	0.92	16.20	0.28	7.08	0.34	3.72	0.11	2.08	0.18	1.51	0.17	4.28	0.18	1.1	2.0	9.8	100.00
4	54.86	0.93	16.33	0.28	7.05	0.33	3.75	0.11	2.04	0.18	1.69	0.18	4.30	0.18	1.1	2.0	8.7	100.00
5	54.50	0.93	16.17	0.28	6.78	0.33	3.73	0.11	1.99	0.18	1.55	0.17	4.33	0.18	1.1	2.0	9.7	100.00
6	55.05	0.93	16.23	0.28	6.81	0.33	3.72	0.11	2.15	0.18	1.61	0.17	4.33	0.18	1.1	2.0	8.8	100.00
7	54.54	0.93	16.37	0.28	7.09	0.33	3.79	0.11	2.07	0.18	1.70	0.18	4.29	0.18	1.1	2.0	8.9	100.00

8	55.11	0.93	16.37	0.28	6.96	0.33	3.72	0.11	1.98	0.18	1.71	0.18	4.38	0.18	1.1	2.0	8.5	100.00
9	54.80	0.93	16.36	0.28	6.83	0.33	3.74	0.11	2.08	0.18	1.64	0.17	4.33	0.18	1.1	2.0	8.9	100.00
10	54.86	0.93	16.17	0.28	7.09	0.33	3.71	0.11	1.99	0.17	1.74	0.18	4.33	0.18	1.1	2.0	8.8	100.00
11	55.11	0.93	16.30	0.28	7.00	0.33	3.78	0.11	2.06	0.18	1.67	0.18	4.24	0.18	1.1	2.0	8.5	100.00
12	54.52	0.93	16.39	0.28	6.97	0.33	3.85	0.11	2.02	0.18	1.59	0.17	4.39	0.18	1.1	2.0	9.0	100.00
13	54.31	0.93	16.26	0.28	7.04	0.33	3.73	0.11	2.08	0.18	1.56	0.17	4.28	0.18	1.1	2.0	9.4	100.00
14	55.70	0.94	16.32	0.28	7.02	0.33	3.75	0.11	1.95	0.18	1.69	0.18	4.31	0.18	1.1	2.0	8.0	100.00
15	54.57	0.93	16.47	0.28	7.01	0.33	3.71	0.11	2.04	0.18	1.54	0.17	4.30	0.18	1.1	2.0	9.1	100.00
Ave.	54.7	0.9	16.3	0.3	7.0	0.3	3.7	0.1	2.0	0.2	1.6	0.2	4.3	0.2	1.1	2.0	9.0	100.0
std	0.5	0.0	0.1	0.0	0.1	0.0	0.0	0.0	0.1	0.0	0.1	0.0	0.0	0.0	0.0	0.0	0.5	0.0
2wt % F glass	SiO_2	+/-	Al_2O_3	+/-	Na_2O	+/-	K_2O	+/-	Ag_2O	+/-	P_2O_5	+/-	F	+/-	Li_2O	B_2O_3	H_2O	Total
1	55.90	0.94	16.79	0.29	6.83	0.33	3.88	0.11	0.58	0.11	1.64	0.18	2.03	0.14	1.1	2.0	10.1	100.00
2	56.61	0.95	16.69	0.28	7.04	0.33	3.99	0.11	0.61	0.11	1.66	0.18	2.06	0.14	1.1	2.0	9.1	100.00
3	56.06	0.94	16.64	0.28	6.97	0.33	3.89	0.11	0.49	0.10	1.55	0.17	2.12	0.14	1.1	2.0	10.1	100.00
4	56.11	0.94	16.68	0.28	7.04	0.33	3.78	0.11	0.52	0.10	1.58	0.17	2.19	0.14	1.1	2.0	9.9	100.00
5	56.57	0.94	16.83	0.28	7.04	0.33	3.87	0.11	0.49	0.10	1.56	0.17	2.16	0.14	1.1	2.0	9.3	100.00
6	56.69	0.95	16.66	0.28	6.96	0.33	3.92	0.11	0.57	0.11	1.59	0.17	2.08	0.14	1.1	2.0	9.3	100.00
7	56.27	0.94	16.71	0.28	6.97	0.33	3.98	0.11	0.49	0.10	1.64	0.18	2.22	0.14	1.1	2.0	9.6	100.00
8	56.19	0.94	16.86	0.28	7.06	0.33	3.87	0.11	0.53	0.10	1.63	0.18	2.23	0.14	1.1	2.0	9.5	100.00
9	55.83	0.94	16.82	0.29	7.24	0.33	3.86	0.11	0.55	0.11	1.56	0.17	2.17	0.14	1.1	2.0	9.8	100.00
10	55.74	0.94	16.82	0.29	7.16	0.33	3.90	0.11	0.53	0.11	1.73	0.18	2.18	0.14	1.1	2.0	9.7	100.00
11	56.31	0.94	16.64	0.28	7.07	0.33	3.91	0.11	0.49	0.10	1.75	0.18	2.13	0.14	1.1	2.0	9.5	100.00
12	56.52	0.94	16.71	0.28	7.14	0.33	3.91	0.11	0.55	0.10	1.67	0.18	2.12	0.14	1.1	2.0	9.2	100.00
13	55.54	0.93	16.69	0.28	7.13	0.33	3.88	0.11	0.59	0.11	1.60	0.17	2.09	0.14	1.1	2.0	10.3	100.00
14	55.74	0.94	16.83	0.28	7.04	0.33	3.86	0.11	0.50	0.10	1.65	0.18	2.15	0.14	1.1	2.0	10.0	100.00
15	56.43	0.94	16.57	0.28	7.22	0.33	3.92	0.11	0.51	0.11	1.58	0.17	2.15	0.14	1.1	2.0	9.4	100.00
Ave.	56.2	0.9	16.7	0.3	7.1	0.3	3.9	0.1	0.5	0.1	1.6	0.2	2.1	0.1	1.1	2.0	9.7	100.0

std	0.4	0.0	0.1	0.0	0.1	0.0	0.1	0.0	0.0	0.0	0.1	0.0	0.1	0.0	0.0	0.0	0.4	0.0
0wt % F glass	SiO_2	+/-	Al_2O_3	+/-	Na_2O	+/-	K_2O	+/-	Ag_2O	+/-	P_2O_5	+/-	F	+/-	*Li_2O*	*B_2O_3*	*H_2O*	Total
1	57.26	0.94	16.91	0.28	7.11	0.33	3.96	0.11	-0.01	-0.02	1.57	0.17	-0.01	-0.02	1.1	2.0	10.1	100.00
2	57.51	0.95	16.84	0.28	7.19	0.33	3.92	0.11	0.03	0.06	1.51	0.17	-0.01	-0.02	1.1	2.0	9.9	100.00
3	57.61	0.95	16.72	0.28	7.14	0.33	3.91	0.11	0.00	0.06	1.65	0.18	0.00	0.09	1.1	2.0	9.9	100.00
4	56.45	0.94	17.01	0.29	7.32	0.33	3.91	0.11	0.00	0.06	1.61	0.17	-0.01	-0.02	1.1	2.0	10.6	100.00
5	57.86	0.95	17.08	0.29	7.21	0.33	3.95	0.11	0.02	0.06	1.55	0.17	-0.01	-0.04	1.1	2.0	9.2	100.00
6	57.67	0.95	17.18	0.29	7.12	0.33	4.00	0.11	0.00	-0.01	1.66	0.18	0.00	-0.01	1.1	2.0	9.3	100.00
7	57.57	0.95	17.00	0.29	7.26	0.33	3.96	0.11	-0.03	-0.09	1.65	0.18	-0.01	-0.03	1.1	2.0	9.5	100.00
8	56.92	0.94	17.08	0.29	7.28	0.33	3.99	0.11	0.00	0.06	1.62	0.17	0.01	0.09	1.1	2.0	10.0	100.00
9	56.92	0.94	17.02	0.29	7.45	0.34	3.97	0.11	-0.01	-0.02	1.54	0.17	-0.01	-0.03	1.1	2.0	10.0	100.00
10	57.85	0.95	16.95	0.29	7.22	0.33	3.94	0.11	0.02	0.06	1.52	0.17	-0.01	-0.04	1.1	2.0	9.4	100.00
11	57.79	0.95	16.97	0.29	7.26	0.33	3.95	0.11	0.02	0.06	1.61	0.17	0.00	0.00	1.1	2.0	9.3	100.00
12	57.52	0.95	17.13	0.29	7.43	0.33	3.95	0.11	-0.01	-0.02	1.61	0.17	0.00	0.00	1.1	2.0	9.3	100.00
13	57.70	0.95	17.06	0.29	7.27	0.33	3.92	0.11	0.02	0.05	1.60	0.17	-0.01	-0.03	1.1	2.0	9.3	100.00
14	57.84	0.95	16.88	0.29	7.16	0.33	3.98	0.11	-0.02	-0.07	1.66	0.18	0.00	-0.01	1.1	2.0	9.4	100.00
15	57.26	0.95	16.93	0.29	7.34	0.33	3.95	0.11	0.01	0.06	1.53	0.17	-0.01	-0.04	1.1	2.0	9.9	100.00
Ave.	57.4	0.9	17.0	0.3	7.3	0.3	4.0	0.1	0.0	0.0	1.6	0.2	0.0	0.0	1.1	2.0	9.7	100.0
std	0.4	0.0	0.1	0.0	0.1	0.0	0.0	0.0	0.0	0.1	0.1	0.0	0.0	0.0	0.0	0.0	0.4	0.0

Trace element contents in the run glasses

High and low temperature analysis to measure trace contents was done at CANMET laboratory, Ottawa, Ontario, Canada.

- Acc. V : 15 kV; current: 60 nA, beam defocused at 5 microns; counting times 60 seconds on peak and background.
- the concentrations of the major elements for the corresponding glass composition were entered as fixed entries for proper calculation of the matrix correction
- Uncertainty represents 3 times the standard deviation based on counting statistics.

6 wt. % F 1000 C°	**MnO**	**+/-**	**Nb_2O_5**	**+/-**	**MnO**	**+/-**	**Ta_2O_5**	**+/-**
1	0.98	0.06	3.20	0.10	0.93	0.05	6.04	0.14
2	0.98	0.05	3.27	0.10	0.94	0.05	5.97	0.14
3	0.96	0.06	3.30	0.10	0.94	0.05	5.91	0.14
4	0.97	0.05	3.36	0.10	0.91	0.05	5.87	0.13
5	0.99	0.06	3.27	0.10	0.95	0.05	5.95	0.14
6	0.95	0.05	3.28	0.10	0.91	0.05	5.73	0.13
7	0.94	0.05	3.28	0.10	0.93	0.05	5.77	0.13
8	0.97	0.05	3.27	0.10	0.94	0.05	5.96	0.14
Ave.	0.97	0.05	3.28	0.10	0.93	0.05	5.90	0.14
std	0.02	0.01	0.04	0.00	0.01	0.00	0.11	0.01
6 wt. % F 800 C°	**MnO**	**+/-**	**Nb_2O_5**	**+/-**	**MnO**	**+/-**	**Ta_2O_5**	**+/-**
1	0.27	0.04	0.77	0.06	0.47	0.04	2.36	0.10
2	0.30	0.04	0.78	0.06	0.48	0.04	2.49	0.10
3	0.33	0.04	0.77	0.06	0.46	0.04	2.40	0.10
4	0.36	0.04	0.73	0.05	0.47	0.04	2.44	0.10
5	0.29	0.04	0.73	0.05	0.47	0.04	2.46	0.10

6	0.28	0.04	0.75	0.06	0.45	0.04	2.40	0.10
7	0.34	0.04	0.70	0.05	0.45	0.04	2.38	0.10
8	0.27	0.04	0.67	0.05	0.47	0.04	2.50	0.10
Ave.	0.31	0.04	0.74	0.06	0.47	0.04	2.43	0.10
std	0.03	0.00	0.04	0.01	0.01	0.00	0.05	0.00
0 wt. % F 1000 C°	**MnO**	**+/-**	**Nb_2O_5**	**+/-**	**MnO**	**+/-**	**Ta_2O_5**	**+/-**
1	0.92	0.05	3.23	0.10	0.97	0.05	6.14	0.14
2	1.02	0.06	3.15	0.10	1.00	0.05	6.17	0.14
3	0.96	0.05	3.18	0.10	1.00	0.05	6.11	0.14
4	0.95	0.05	3.11	0.10	0.96	0.05	6.09	0.14
5	0.96	0.05	3.22	0.10	0.96	0.05	6.22	0.14
6	0.93	0.05	3.22	0.10	0.95	0.05	6.12	0.14
7	0.91	0.05	3.19	0.10	0.96	0.05	6.14	0.14
8	0.97	0.06	3.24	0.10	0.95	0.05	6.05	0.14
Ave.	0.95	0.05	3.19	0.10	0.97	0.05	6.13	0.14
std	0.03	0.00	0.04	0.00	0.02	0.00	0.05	0.00

0 wt. % F 800 C°	MnO	+/-	Nb_2O_5	+/-	MnO	+/-	Ta_2O_5	+/-
1	0.32	0.04	0.87	0.06	0.47	0.04	2.47	0.10
2	0.38	0.04	0.81	0.06	0.47	0.04	2.39	0.10
3	0.31	0.04	0.89	0.06	0.46	0.04	2.36	0.10
4	0.33	0.04	0.92	0.06	0.46	0.04	2.47	0.10
5	0.33	0.04	0.86	0.06	0.45	0.04	2.39	0.10
6	0.33	0.04	0.85	0.06	0.47	0.04	2.47	0.10
7	0.33	0.04	0.84	0.06	0.47	0.04	2.39	0.10
8	0.34	0.04	0.85	0.06	0.46	0.04	2.36	0.10
Ave.	0.33	0.04	0.86	0.06	0.46	0.04	2.41	0.10
std	0.02	0.00	0.03	0.00	0.01	0.00	0.05	0.00

6 wt. % F 1000 C°	ZrO_2	+/-	HfO_2	+/-
1	0.98	0.06	1.97	0.09
2	0.94	0.06	1.95	0.09
3	0.95	0.06	1.81	0.09
4	0.95	0.06	1.87	0.09
5	0.89	0.06	1.98	0.09
6	0.93	0.06	1.99	0.09
7	0.94	0.06	1.99	0.09
8	0.93	0.06	1.83	0.09
Ave.	0.94	0.06	1.92	0.09
std	0.03	0.00	0.08	0.00

6 wt. % F 800 C°	**ZrO_2**	**+/-**	**HfO_2**	**+/-**
1	0.39	0.04	0.76	0.07
2	0.39	0.04	0.76	0.07
3	0.42	0.04	0.76	0.07
4	0.39	0.04	0.76	0.07
5	0.41	0.04	0.83	0.07
6	0.39	0.04	0.98	0.07
7	0.39	0.04	0.98	0.07
8	0.40	0.04	0.93	0.07
Ave.	0.40	0.04	0.85	0.07
std	0.01	0.00	0.10	0.00
0 wt. % F 1000 C°	**ZrO_2**	**+/-**	**HfO_2**	**+/-**
1	0.68	0.05	1.55	0.08
2	0.65	0.05	1.55	0.08
3	0.64	0.05	1.74	0.09
4	0.63	0.05	1.53	0.08
5	0.64	0.05	1.53	0.08
6	0.69	0.05	1.78	0.08
7	0.62	0.05	1.58	0.08
8	0.66	0.05	1.68	0.08
Ave.	0.65	0.05	1.62	0.08
std	0.02	0.00	0.10	0.00

6 wt. % F 1000 C°	ZrO_2	+/-	HfO_2	+/-
1	0.25	0.03	0.97	0.07
2	0.26	0.03	1.09	0.08
3	0.24	0.03	0.99	0.08
4	0.23	0.03	0.98	0.08
5	0.23	0.03	1.00	0.08
6	0.25	0.03	1.08	0.08
7	0.23	0.03	1.08	0.08
8	0.23	0.03	1.10	0.08
Ave.	0.35	0.027	1.09	0.021
std	0.38	0.000	1.07	0.000

Appendix B

Trace element concentrations

The concentrations of the trace elements were measured using Cameca SX50 electron microprobe at University of Toronto, Toronto, Ontario, Canada. The conditions and the standers were used in this analysis are given in the lab report:

"TakeOff = 40.0 KiloVolt = 15.0 Beam Current = 60.0 Beam Size = 5

(Magnification (analytical) = 400), Beam Mode = Analog Spot

(Magnification (default) = 400, Magnification (imaging) = 400)

Image Shift (X,Y): 0, 0

Compositional analyses were acquired on an electron microprobe equipped with 3 tunable wavelength dispersive spectrometers. Operating conditions were 40 degrees takeoff angle, and a beam energy of 15 keV. The beam current was 60 nA, and the beam diameter was 5 microns. Elements were acquired using analyzing crystals LiF for W la, Ta la, Hf la, Mn ka, PET for Nb la, K ka, Zr la, Ag la, P ka, and TAP for Al ka, Si ka, Na ka, F ka. The standards were Tasx1 for Ta la, NaNbO3sx1 for Nb la, Na ka, bustamsx1 for Mn ka, HfSiO4sx2 for Hf la, ZrSiO4sx2 for Zr la, obsUA_GlassesSX5/5 for Si ka, K ka, Al ka, CaF2_GlassesSX50/5 for F ka, and apatsx1 for P ka.

The counting time was 6 seconds for Na ka, K ka, F ka, 10 seconds for Al ka, Si ka, P ka, Mn ka, and 60 seconds for Ta la, Nb la, Hf la, Zr la, Ag la, W la. The off peak counting time was 6 seconds for Na ka, K ka, F ka, 10 seconds for Al ka, Si ka, P ka, Mn ka, and 60 seconds for Ta la, Nb la, Hf la, Zr la, Ag la, W la.

The off peak correction method was Linear for all elements. Unknown and standard intensities were corrected for deadtime. Oxygen was calculated by cation stoichiometry and included in the matrix correction. Oxygen equivalent from halogens (F/Cl/Br/I), was subtracted in the matrix correction. The matrix correction method was ZAF or Phi-Rho-Z calculations and the mass absorption coefficients dataset was CITZMU Heinrich (1966) and Henke and Ebisu (1974). The ZAF or Phi-Rho-Z algorithm utilized was Armstrong/Love Scott (default). See J. T. Armstrong, Quantitative analysis of silicates and oxide minerals: Comparison of Monte-Carlo, ZAF and Phi-Rho-Z procedures, Microbeam Analysis--1988, p 239-246" (Yanan Liu, probe operator, Department of Geology, University of Toronto)

The concentration of trace element oxides (wt.%) and the detection limits (D.L.) are given in the following tables:

0 wt. % F glass	**MnO**	**Mn D.L.**	**Nb_2O_5**	**Nb D.L.**	**MnO**	**MnO D.L.**	**Ta_2O_5**	**Ta D.L.**	**Zr_2O**	**Zr D.L**	**Hf_2O**	**Hf D.L.**
1	0.34	0.023	1.04	0.020	0.49	0.028	2.70	0.055	0.19	0.024	0.85	0.048
2	0.33	0.026	0.97	0.019	0.51	0.028	2.90	0.061	0.23	0.019	0.83	0.051
3	0.36	0.028	1.05	0.021	0.50	0.026	2.90	0.055	0.28	0.022	0.87	0.048
4	0.34	0.027	1.06	0.021	0.48	0.027	2.56	0.054	0.26	0.022	0.85	0.048
5	0.32	0.027	1.06	0.021	0.57	0.025	2.73	0.056	0.27	0.023	0.86	0.049
6	0.33	0.027	1.02	0.019	0.54	0.025	2.88	0.055	0.22	0.022	0.84	0.048
7	0.31	0.027	1.06	0.020	0.52	0.026	2.78	0.056	0.27	0.022	0.89	0.048

8	0.36	0.026	0.99	0.021	0.46	0.026	2.71	0.055	0.25	0.023	0.80	0.049
9	0.35	0.027	1.09	0.021	0.51	0.025	2.76	0.055	0.24	0.022	0.88	0.049
10	0.38	0.000	1.07	0.000	0.47	0.027	2.64	0.056	0.29	0.000	0.90	0.000
11	0.36	0.023	1.03	0.020	0.56	0.026	2.94	0.056	0.25	0.023	0.89	0.048
12	0.36	0.025	1.02	0.020	0.49	0.027	2.72	0.055	0.34	0.023	0.77	0.048
13	0.39	0.027	1.01	0.020	0.52	0.028	2.90	0.055	0.21	0.021	0.81	0.047
14	0.34	0.025	1.03	0.021	0.65	0.026	2.76	0.056	0.26	0.024	0.81	0.048
15	0.00	0.025	0.00	0.020	0.50	0.027	2.62	0.055	0.25	0.022	0.96	0.047
Ave.	0.32	0.02	0.97	0.02	0.52	0.03	2.77	0.06	0.25	0.02	0.85	0.05
std	0.09	0.01	0.27	0.01	0.05	0.00	0.12	0.00	0.04	0.01	0.05	0.01
2 wt. % F glass	**MnO**	**Mn D.L.**	**Nb_2O_5**	**Nb D.L.**	**MnO**	**MnO D.L.**	**Ta_2O_5**	**Ta D.L.**	**Zr_2O**	**Zr D.L**	**Hf_2O**	**Hf D.L.**
1	0.34	0.027	1.04	0.021	0.49	0.026	2.70	0.057	0.19	0.024	0.85	0.048
2	0.33	0.026	0.97	0.020	0.51	0.026	2.90	0.055	0.23	0.019	0.83	0.051
3	0.36	0.026	1.05	0.020	0.50	0.027	2.90	0.054	0.28	0.022	0.87	0.048
4	0.34	0.026	1.06	0.021	0.48	0.026	2.56	0.055	0.26	0.022	0.85	0.048
5	0.32	0.025	1.06	0.019	0.57	0.027	2.73	0.056	0.27	0.023	0.86	0.049
6	0.33	0.027	1.02	0.021	0.54	0.026	2.88	0.056	0.22	0.022	0.84	0.048
7	0.31	0.026	1.06	0.020	0.52	0.025	2.78	0.056	0.27	0.022	0.89	0.048
8	0.36	0.026	0.99	0.021	0.46	0.027	2.71	0.055	0.25	0.023	0.80	0.049
9	0.35	0.027	1.09	0.023	0.51	0.026	2.76	0.054	0.24	0.022	0.88	0.049
10	0.38	0.024	1.07	0.021	0.47	0.027	2.64	0.055	0.29	0.000	0.90	0.000
11	0.36	0.025	1.03	0.019	0.56	0.025	2.94	0.055	0.25	0.023	0.89	0.048
12	0.36	0.026	1.02	0.021	0.49	0.025	2.72	0.055	0.34	0.023	0.77	0.048
13	0.39	0.027	1.01	0.021	0.52	0.027	2.90	0.054	0.21	0.021	0.81	0.047
14	0.34	0.026	1.03	0.021	0.65	0.024	2.76	0.054	0.26	0.024	0.81	0.048
15	0.00	0.028	0.00	0.021	0.50	0.028	2.62	0.056	0.25	0.022	0.96	0.047

Ave.	0.32	0.03	0.97	0.02	0.52	0.03	2.77	0.06	0.25	0.02	0.85	0.05
std	0.09	0.00	0.27	0.00	0.05	0.00	0.12	0.00	0.04	0.01	0.05	0.01

4 wt. % F glass	**MnO**	**Mn D.L.**	**Nb_2O_5**	**Nb D.L.**	**MnO**	**MnO D.L.**	**Ta_2O_5**	**Ta D.L.**	**Zr_2O**	**Zr D.L**	**Hf_2O**	**Hf D.L.**
1	0.34	0.027	1.04	0.020	0.49	0.028	2.70	0.055	0.19	0.024	0.85	0.048
2	0.33	0.026	0.97	0.021	0.51	0.026	2.90	0.057	0.23	0.019	0.83	0.051
3	0.36	0.026	1.05	0.021	0.50	0.025	2.90	0.054	0.28	0.022	0.87	0.048
4	0.34	0.026	1.06	0.021	0.48	0.024	2.56	0.055	0.26	0.022	0.85	0.048
5	0.32	0.027	1.06	0.021	0.57	0.025	2.73	0.056	0.27	0.023	0.86	0.049
6	0.33	0.025	1.02	0.020	0.54	0.027	2.88	0.056	0.22	0.022	0.84	0.048
7	0.31	0.025	1.06	0.021	0.52	0.025	2.78	0.055	0.27	0.022	0.89	0.048
8	0.36	0.026	0.99	0.020	0.46	0.025	2.71	0.055	0.25	0.023	0.80	0.049
9	0.35	0.027	1.09	0.021	0.51	0.027	2.76	0.056	0.24	0.022	0.88	0.049
10	0.38	0.026	1.07	0.019	0.47	0.025	2.64	0.053	0.29	0.000	0.90	0.000
11	0.36	0.025	1.03	0.021	0.56	0.026	2.94	0.056	0.25	0.023	0.89	0.048
12	0.36	0.027	1.02	0.022	0.49	0.028	2.72	0.055	0.34	0.023	0.77	0.048
13	0.39	0.027	1.01	0.020	0.52	0.027	2.90	0.055	0.21	0.021	0.81	0.047
14	0.34	0.027	1.03	0.020	0.65	0.028	2.76	0.055	0.26	0.024	0.81	0.048
15	0.00	0.026	0.00	0.020	0.50	0.028	2.62	0.057	0.25	0.022	0.96	0.047
Ave.	0.32	0.03	0.97	0.02	0.52	0.03	2.77	0.06	0.25	0.02	0.85	0.05
std	0.09	0.00	0.27	0.00	0.05	0.00	0.12	0.00	0.04	0.01	0.05	0.01
6 wt. % F glass	**MnO**	**Mn D.L.**	**Nb_2O_5**	**Nb D.L.**	**MnO**	**MnO D.L.**	**Ta_2O_5**	**Ta D.L.**	**Zr_2O**	**Zr D.L**	**Hf_2O**	**Hf D.L.**
1	0.34	0.028	1.04	0.020	0.49	0.027	2.70	0.055	0.19	0.024	0.85	0.048

2	0.33	0.026	0.97	0.020	0.51	0.027	2.90	0.054	0.23	0.019	0.83	0.051
3	0.36	0.025	1.05	0.019	0.50	0.027	2.90	0.055	0.28	0.022	0.87	0.048
4	0.34	0.024	1.06	0.020	0.48	0.027	2.56	0.055	0.26	0.022	0.85	0.048
5	0.32	0.025	1.06	0.021	0.57	0.026	2.73	0.055	0.27	0.023	0.86	0.049
6	0.33	0.027	1.02	0.021	0.54	0.027	2.88	0.055	0.22	0.022	0.84	0.048
7	0.31	0.025	1.06	0.021	0.52	0.027	2.78	0.090	0.27	0.022	0.89	0.048
8	0.36	0.025	0.99	0.020	0.46	0.027	2.71	0.085	0.25	0.023	0.80	0.049
9	0.35	0.027	1.09	0.020	0.51	0.024	2.76	0.087	0.24	0.022	0.88	0.049
10	0.38	0.025	1.07	0.020	0.47	0.027	2.64	0.089	0.29	0.000	0.90	0.000
11	0.36	0.026	1.03	0.020	0.56	0.027	2.94	0.090	0.25	0.023	0.89	0.048
12	0.36	0.028	1.02	0.020	0.49	0.027	2.72	0.079	0.34	0.023	0.77	0.048
13	0.39	0.027	1.01	0.020	0.52	0.025	2.90	0.090	0.21	0.021	0.81	0.047
14	0.34	0.028	1.03	0.020	0.65	0.025	2.76	0.091	0.26	0.024	0.81	0.048
15	0.00	0.028	0.00	0.020	0.50	0.044	2.62	0.078	0.25	0.022	0.96	0.047
Ave.	0.32	0.03	0.97	0.02	0.52	0.03	2.77	0.07	0.25	0.02	0.85	0.05
std	0.09	0.00	0.27	0.00	0.05	0.00	0.12	0.02	0.04	0.01	0.05	0.01

Trace elements compositions of Al-rich experiments were measured by Cambax MBX microprobe at Carleton University, Ottawa, Canada.

6wt. % AlF_3 glass	**MnO**	**Mn D.L.**	**Nb_2O_5**	**Nb D.L.**	**MnO**	**MnO D.L.**	**Ta_2O_5**	**Ta D.L.**	**Hf_2O**	**Hf D.L**
1	0.09	0.01	0.27	0.02	0.27	0.01	1.71	0.05	0.055	0.05
2	0.15	0.01	0.39	0.02	0.21	0.01	1.37	0.05	0.057	0.05
3	0.18	0.01	0.42	0.02	0.21	0.01	1.34	0.05	0.054	0.05
4	0.19	0.01	0.40	0.02	0.23	0.01	1.48	0.05	0.055	0.05

5	0.14	0.01	0.37	0.02	0.23	0.01	1.32	0.05	0.056	0.04
6	0.16	0.01	0.40	0.02	0.22	0.01	1.51	0.05	0.056	0.05
7	0.15	0.01	0.41	0.02	0.21	0.01	1.28	0.05	0.055	0.04
8	0.15	0.01	0.40	0.02	0.19	0.01	1.36	0.05	0.055	0.05
9	0.15	0.01	0.42	0.02	0.23	0.01	1.25	0.05	0.056	0.05
Ave.	0.15	0.01	0.39	0.02	0.22	0.01	1.40	0.05	0.06	0.05
std	0.03	0.00	0.05	0.00	0.02	0.00	0.14	0.00	0.00	0.00